Analytical Methods for Realistic Cosmic Strings



Pedro Belo Barbosa
Master in Astronomy and Astrophysics
Department of Physics and Astronomy
Faculty of Sciences of the University of Porto
2025

Analytical Methods for Realistic Cosmic Strings

Pedro Belo Barbosa
Dissertation carried out as part of the Master
in Astronomy and Astrophysics
Department of Physics and Astronomy
2025

Supervisor
Dr. Carlos Martins, Main Researcher, Center for Astrophysics of the University of Porto, Faculty of Sciences





Acknowledgments

I want to thank my supervisor, Dr. Carlos Martins, for the many valuable discussions that provided essential insight into the topics covered in this thesis, and for the opportunities he gave me to present parts of my work.

A word of appreciation to all my friends who have been with me since the beginning of these long—yet somehow short—five years, namely Eduardo Gonçalves, João Magalhães, Ricardo Elísio, Pedro Malta, Mário Alves, Luciano Santos, Bruno Pereira, João Brites, Luís Magalhães, Ricardo Vilhena, David Paula and Guilherme Conde.

Above all, I would like to thank my parents and my two brothers. Their unwavering support and love have shaped who I am, and I owe them more than words can express.

I also acknowledge that this work was financed by Portuguese funds through FCT in the framework of the project 2022.04048.PTDC (Phi in the Sky, DOI 10.54499/2022.04048.PTDC).

Resumo

Cordas cósmicas são defeitos topológicos que se espera que surjam em vários cenários cosmológicos, à medida que a temperatura do Universo diminui e este passa por uma sequência de transições de fase com quebras de simetria. Embora estes objetos ainda não tenham sido observados — seja direta ou indiretamente —, a sua deteção proporcionaria uma perceção valiosa sobre a física de altas energias que moldou o Universo primordial. Por outro lado, descartá-los exigiria uma revisão substancial da nossa compreensão atual destes processos fundamentais.

No esforço de procurar assinaturas de cordas cósmicas, modelos teóricos robustos são essenciais para interpretar dados observacionais. Embora tais modelos possam surgir da teoria de campo e de simulações numéricas, eles enfrentam desafios significativos. Uma das principais dificuldades decorre da vasta gama de escalas de comprimento e de tempo envolvidas na evolução das cordas cósmicas, tornando o tratamento numérico completo extremamente exigente. Como resultado, modelos fenomenológicos foram desenvolvidos para capturar o comportamento macroscópico das redes de cordas. Entre estes, o modelo de Uma Escala dependente da Velocidade, VOS, destaca-se por tratar a rede como um sistema termodinâmico, caracterizando as suas propriedades principais e prevendo a sua evolução em larga escala.

Extensões deste quadro teórico têm em conta cordas cósmicas supercondutoras, que transportam correntes internas e possuem graus de liberdade adicionais. Estas são bem descritas pelo modelo de Uma Escala dependente da Carga e da Velocidade, CVOS, uma generalização do formalismo VOS. Uma característica central de ambos os modelos é a formação de laços, que atua como o principal mecanismo de perda de energia da rede.

Nesta dissertação, procurámos inicialmente compreender como laços supercondutores evoluem sob várias condições, considerando diferentes taxas de expansão e modelos físicos. Analisámos o papel desempenhado pela carga interna e pela corrente na sua dinâmica. Mais adiante, propomos um novo mecanismo que, em princípio, permite à rede de cordas cósmicas ganhar energia. Consideramos cordas cósmicas com corrente sujeitas a um campo magnético externo, e investigamos como esta interação influencia a evolução da rede. Desenvolvemos um formalismo matemático que estende o modelo CVOS e analisamos as suas soluções estáveis em tempos tardios. Estas soluções visam descrever o comportamento em larga escala da rede de cordas, enquanto restringem propriedades do campo magnético envolvente.

Palavras-chave: Cosmologia, Defeitos Topológicos, Cordas Supercondutoras, Modelos Analíticos, CVOS

Abstract

Cosmic strings are topological defects expected to emerge in various cosmological scenarios, as the temperature of the Universe decreases and it undergoes a sequence of symmetry-breaking phase transitions. Although these objects have not yet been observed—either directly or indirectly—their detection would provide valuable insight into the high-energy physics that shaped the early Universe. Conversely, ruling them out would require a substantial revision of our current understanding of these fundamental processes.

In the effort to search for cosmic string signatures, robust theoretical models are essential for interpreting observational data. While such models may arise from field theory and numerical simulations, they face significant challenges. One major difficulty stems from the vast range of length and time scales involved in the evolution of cosmic strings, making full numerical treatment extremely demanding. As a result, phenomenological models have been developed to capture the macroscopic behavior of string networks. Among these, the Velocity dependent One-Scale model (VOS) model stands out for treating the network as a thermodynamic system, characterizing its key properties and predicting its large-scale evolution.

Extensions of this framework account for superconducting cosmic strings, which carry internal currents and possess additional degrees of freedom. These are well described by the Charge-Velocity dependent One-Scale model (CVOS), a generalization of the VOS formalism. A central feature of both models is loop formation, which acts as the primary energy loss mechanism of the network.

In this dissertation, we first aimed to understand how superconducting loops evolve under various conditions, considering different expansion rates and physical models. We analyzed the role played by the internal charge and current in shaping their dynamics. Later, we propose a novel mechanism that, in principle, allows the cosmic string network to gain energy. We consider current-carrying cosmic strings subjected to an external magnetic field, and investigate how this interaction influences the evolution of the network. We develop a mathematical formalism extending the CVOS model and analyze its late-time stable solutions. These solutions aim to describe the large-scale behavior of the string network while simultaneously placing constraints on the properties of the ambient magnetic field.

Keywords: Cosmology, Topological Defects, Superconducting Strings, Analytic Models, CVOS

Contents

List of Figures vii

List of Tables viii

List of Abbreviations ix

1 Introduction to Cosmic Strings 1

1.1 Spontaneous Symmetry Breaking . . . 1

1.2 Cosmic Strings and Others Topological Defects . . . 2

1.2.1 Abelian-Higgs Model . . . 3

1.3 Current-Carrying Strings . . . 4

1.4 Effective Actions . . . 5

1.4.1 Nambu-Goto Strings . . . 5

1.4.2 Effective Action for Superconducting Strings . . . 6

1.5 Loop formation . . . 7

2 Cosmic String Evolution 8

2.1 VOS . . . 8

2.1.1 Energy Loss Terms . . . 12

2.2 CVOS . . . 12

3 Circular Loops 17

3.1 Loop Configuration and Microscopic Equations . . . 17

3.2 Loop Evolution . . . 20

3.2.1 The Linear Model . . . 20

3.2.2 Kaluza-Klein vs Witten Models . . . 22

4 Cosmic Strings Evolution in the Presence of an External Magnetic Field 26

4.1 The Model . . . 26

4.2 Macroscopic Evolution . . . 29

4.3 Scaling Regime . . . 30

4.4 Analytical Solutions . . . 33

4.4.1 $\beta = 0$ and $\eta \geq 0$ . . . 33

4.4.2 $\beta = 0$ and $\eta < 0$ . . . 39

4.4.3 $\beta < 0$ 40

5 Conclusion **48**

References **52**

List of Figures

1.1 When strings intersect they can: a) reconnect, b) not interact at all and c) entangle [10] . . . 7
3.1 From left to right: the first plot represents the radius of the loop in units of conformal time, as function of τ for the different expansion rates. The second and third plots represent the velocity $\dot{r}$ and the total charge y as a function of τ. Blue, orange and green lines correspond to $\lambda = 0$, $\lambda = 1$ and $\lambda = 2$, respectively. . . . 20
3.2 The time needed to complete one oscillation after the radius reaches the first minimum. Blue, orange and green lines correspond to $\lambda = 0$, $\lambda = 1$ and $\lambda = 2$, respectively. . . . 21
3.3 Radius of the loop as a function of time. The dashed black line corresponds to a ring with constant radius r_0. Blue, orange and green lines correspond to $\lambda = 0$, $\lambda = 1$ and $\lambda = 2$, respectively. . . . 22
3.4 Radius of the loop as a function of time. Magnetic and electric regimes are represented on the left and right sides, respectively. The ones above correspond to the Kaluza-Klein model and below to the Witten one. Blue, orange and green lines correspond to $\lambda = 0$, $\lambda = 1$ and $\lambda = 2$, respectively. . . . 23
3.5 Chirality as a function of time. Magnetic and electric regimes are represented on the left and right sides, respectively. The ones above correspond to the Kaluza-Klein model and below to the Witten one. Blue, orange and green lines correspond to $\lambda = 0$, $\lambda = 1$ and $\lambda = 2$, respectively. . . . 24
4.1 Ratio between the bare string energy E_0, and the total energy, E, as a function of the final velocity squared, v_0^2 . . . 35
4.2 Ratio between the bare string energy E_0, and the total energy, E, as a function of the final velocity squared, v_0^2, in the radiation (blue dots) and matter (orange dots) eras, considering solution $A2$. . . . 36
4.3 Possible values of α and ϵ considering the solution $C1$. Regions in gray do not belong to the parameter space. . . . 42
4.4 Possible values of α considering the solution $C2$. Regions in gray do not belong to the parameter space . . . 43
4.5 Possible values of α considering the solution $C4$. Regions in gray do not belong to the parameter space . . . 44

4.6 Possible values of α considering the solution $C5$. Regions in gray do not belong to the parameter space 46
4.7 Possible values of α considering the solution $C6$. 47

List of Tables

5.1 Brief summary of the most important features of the solutions found in section 4. The possible values of λ in the solutions $A1$ and $A2$ were not studied. The λ interval in the $A3$ column corresponds to the case where $\eta > 0$. 49

List of Abbreviations

CVOS Charge-Velocity dependent One-Scale model

VOS Velocity dependent One-Scale model

rms root mean square

Λ**CDM** Lambda Cold Dark Matter

FLRW Friedmann–Lemaître–Robertson–Walker

CMB Cosmic Microwave Background

1 Introduction to Cosmic Strings

It is common knowledge how a single drop of water spreads across a sheet of paper. Equally intuitive is the outcome when two large drops, each of a different color, are absorbed simultaneously. As the stains expand, they eventually collide—provided the paper is small enough or the drops sufficiently large. Suppose one drop is red and the other blue; where they meet, a chaotic, irregular purple line emerges. This boundary may be viewed as a topological defect: a localized disruption in the otherwise ordered pattern of color across the wetted paper.

In fact, a topological defect is a little bit more than that. It consists in the fingerprint left behind by a spontaneous symmetry breaking. In a system invariant under the group G, let H be the subgroup leaving the vacuum expectation value unaltered. The vacuum manifold is then given by the quotient space $G\backslash H$ and denoted by $\mathcal{M}$. Topological features of $\mathcal{M}$, more specifically, its homotopy groups, will determine the geometry of the possible remaining topological structures. For a more detailed discussion see [1, 2].

In this chapter, I will provide a concise overview of the fundamental aspects of cosmic strings. At the same time, I shall begin to introduce key notation and establish conventions that will be used consistently throughout the remainder of this thesis.

1.1 Spontaneous Symmetry Breaking

This idea of spontaneous symmetry breaking was first introduced in condensed matter physics. One example is the isotropic model of a ferromagnet which, although described by a rotationally-invariant Hamiltonian, can develop a magnetic moment pointing in some arbitrary direction [3].

A simple model, which illustrates efficiently these symmetry-breaking phase transitions is the Goldstone one [4]. In this model, the system is described by a complex scalar field ϕ and is given by the following Lagrangian:

$$\mathcal{L} = \partial_\mu \bar{\phi} \partial^\mu \phi - V(\phi) \tag{1.1}$$

where the potential is given by

$$V(\phi) = \frac{1}{4}\lambda \left(\bar{\phi}\phi - \eta^2\right)^2 \tag{1.2}$$

with λ and η being positive constants. This potential has a local maximum for $\phi = 0$ and it decreases as $|\phi| \to \eta$, reaching the minimum. For greater values of the scalar field, the

potential rises again, reminding a mexican hat. This model is invariant under global phase transformations:

$$\phi(x) \to e^{i\alpha}\phi(x). \tag{1.3}$$

Global in the sense that α does not depend on the spacetime coordinates x. Otherwise, we would have a gauge model, which is more common in cosmological particle physics and shall be studied further ahead. A look at Equation 1.2 and at the equation of motion resulting from Equation 1.1,

$$\left[\partial_\mu\partial^\mu + \frac{1}{2}\lambda\left(|\phi|^2 - \eta^2\right)\right]\phi = 0, \tag{1.4}$$

clearly shows that the vacuum state, the one which minimizes the energy, corresponds to $|\phi|^2 = \eta^2$. And therefore it has the form $\phi = \eta e^{i\theta}$, for some real value θ.

The state $\phi = 0$ corresponds to a relative maximum of the potential, and is, therefore, a static solution. It also preserves the symmetry given by expression 1.3. However, it is unstable. We can consider a configuration where the initial state is given by $\phi = 0$. Any perturbation will push the system towards its true vacuum, $\phi = \eta e^{i\theta}$, which clearly does not hold the previous symmetry.

These spontaneous symmetry breaking phase transitions played originally an important role in condensed matter, and later in particle physics and cosmology, and we shall see how they are related to topological defects.

1.2 Cosmic Strings and Others Topological Defects

As previously mentioned, topological defects were first introduced in the context of condensed matter physics. Today, their relevance extends across particle physics and cosmology. Topology, albeit somewhat loosely speaking, concerns itself with the fundamental properties and structures of continuous manifolds. When we speak of topological defects, we refer to regions where this continuity is somehow strained or disrupted. Paradoxically, such 'defective' regions are not arbitrary anomalies, but rather inevitable consequences imposed by the very requirement of continuity itself.

The way they are related to spontaneous symmetry breaking is through the Kibble mechanism [1]. We can take the previous Goldstone model, and assume the scalar field to be real. Now, the vacuum expectation value would be one of two separated points, $\phi = \pm\eta$. 'Separated' meaning that, any path connecting the two vacuum states would force the scalar field

to be excited. When the symmetry-breaking phase transition happens, causally independent points may choose different vacuum state values. So, similarly to the drops of water, where the color of the wet paper had to pass from red to blue, when two regions with different vacuum states encounter each other, the scalar field will have to pass from $-\eta$ to η. In order to do this continuously, there will be a region where $\phi = 0$, recovering the broken symmetry. The kinetic part of Equation 1.1 will try to manage the non-zero field gradient, resulting in a very localized region of energy. If we imagine we are in a three-dimensional space, this region would correspond to a two-dimensional wall, normally called domain wall. This process, through which topological defects are formed, is called the Kibble mechanism.

Domain walls are but one member in the rich family of topological defects. Its members are most readily distinguished by their dimensionality. Point-like defects are known as monopoles, while one-dimensional, line-like configurations are referred to as strings. Domain walls occupy two dimensions, and beyond them lie the most abstract and elusive of all — the three-dimensional textures. In the context of this thesis, however, our attention will be focused exclusively on strings. We shall soon explore how such structures naturally emerge within more realistic physical models.

1.2.1 Abelian-Higgs Model

In a cosmological context, the Abelian-Higgs model is more relevant because it is invariant under gauge transformations, like the ones we think would exist in the beginning of the Universe (such as GUT or the electroweak symmetry). The Lagrangian is given by

$$\mathcal{L} = \bar{D}_\mu \bar{\phi} D^\mu \phi - V(\phi) + \frac{1}{4} F_{\mu\nu} F^{\mu\nu}, \tag{1.5}$$

where ϕ is a charged complex scalar field, $F_{\mu\nu} = \partial_\mu A_\nu - \partial_\nu A_\mu$ and $D_\mu = \partial_\mu - ieA_\mu$. Here, we introduced the gauge fields, A_μ, and a coupling constant e. The potential is the one given by 1.2. The Lagrangian 1.5 is invariant under the gauge transformations:

$$\phi(x) \to e^{i\Lambda(x)} \phi(x) \quad \text{and} \quad A_\mu(x) \to A_\mu(x) + \frac{1}{e} \partial_\mu \Lambda(x), \tag{1.6}$$

where $\Lambda(x)$ is a function of the spacetime coordinates.

Again, the true vacuum corresponds to the state $\phi = \eta e^{i\theta}$. The Nielsen-Olesen vortex [5] is a stable, cylindrical symmetric solution for the equation of motion resulting from Equation 1.5. It consists in a line where the scalar field sits in the relative maximum of the potential, as it could in the Goldstone model. As we move way from the line, ϕ tends to the vacuum expectation value.

If we take a closed path around the vortex, the complex phase of the scalar field will return to its original value, after winding around the minima of the mexican hat potential a number n of times. n is a topological constant and is called the winding number. If $n \neq 0$, then a cosmic string is formed.

1.3 Current-Carrying Strings

Edward Witten showed that cosmic strings could carry extra degrees of freedom. In [6], he demonstrated how superconductivity could arise from a charged Higgs field in the string core or from the zero modes of fermions moving along the string. He also presented several other models with broader symmetry groups, which give rise to superconducting cosmic strings as well. There is a myriad of systems which form this kind of strings.

The most simple one results from a $\mathcal{U}(1)$ symmetry breaking on a system which is invariant under $\mathcal{U}(1) \times \tilde{\mathcal{U}}(1)$. The Lagrangian describing this situation is the following

$$\mathcal{L} = \bar{D}_\mu \bar{\phi} D^\mu \phi + \bar{\tilde{D}}_\mu \bar{\sigma} \tilde{D}^\mu \sigma - V(\phi, \sigma) + \frac{1}{4} F_{\mu\nu} F^{\mu\nu} + \frac{1}{4} \tilde{F}_{\mu\nu} \tilde{F}^{\mu\nu}, \tag{1.7}$$

where ϕ, σ are the complex scalar fields associated with $\mathcal{U}(1)$, $\tilde{\mathcal{U}}(1)$ symmetries, respectively. The covariant derivatives are given by $D_\mu = \partial_\mu - ieA_\mu$ and $\tilde{D}_\mu = \partial_\mu - i\tilde{e}\tilde{A}_\mu$, with e, $\tilde{e}$ being coupling constants. The potential is now defined as

$$V(\phi, \sigma) = \frac{\lambda}{4} \left(|\phi|^2 - \eta^2 \right)^2 + \frac{\tilde{\lambda}}{4} \left(|\sigma|^2 - \tilde{\eta}^2 \right)^2 + g|\phi|^2 |\sigma|^2. \tag{1.8}$$

The constants must obey $\lambda\eta > \tilde{\lambda}\tilde{\eta}$ and $g\eta^2 \geq \frac{1}{4}\tilde{\lambda}\tilde{\eta}^2$, in order to have a broken $\mathcal{U}(1)$ symmetry. This means, it would be more favorable, in energetic terms, to have $|\phi| = \eta$ and $\sigma = 0$. However, in the string, where $\phi = 0$, σ does not need be vanish.

In fact, we can imagine the value of the condensate in the string to be σ_0. So, any additional complex phase will not alter the system, and therefore, $\sigma = \sigma_0(x, y)\, e^{i\theta(z,t)}$ in the string. The string was considered to be lying in the z direction. However, we can view the coordinate z as a parameterization of the string, and x, y to parameterize the normal plane to the string.

Similarly to the complex phase winding around the potential in the previous section, the value of θ, as we move along a string loop, and arrive at the same place, can differ from the initial value by an integer number, N, times 2π

$$N = \frac{1}{2\pi} \oint dz \frac{d\theta}{dz}. \tag{1.9}$$

This is a topological constant. Witten showed how perturbations in the σ value can give

origin to a current within the string [6]. This current would be proportional to N, and therefore, constant. And so, we would have current-carrying strings.

1.4 Effective Actions

The previous Lagrangians provide a way to study the microphysics of the strings. This field theory approach can lead to a detailed picture about core structure and geometry, the interactions and certain energy loss mechanisms. However, the equations are incredibly cumbersome and very difficult to analyze analytically. Even numerically things are not easier. This is due to the large range of length scales relevant for cosmic strings. The radius of the string can be estimated to be of order 10^{-32}cm, for strings formed at GUT scales, while their length is comparable to the Hubble radius. This brings difficulties when we analyze them numerically, although there are an immense number of cosmic strings simulations [7, 8].

However, this length scale range problem is like a knife with two edges. All because, when we are looking at a string network, at a cosmic scale, their appear to be one-dimensional. And in fact, it is expected that the degrees of freedom within the core of the strings to not influence the large scale evolution. In this section, we shall see how we can reduce the Lagrangian to a $1+1$ dimensional problem, by introducing the Nambu-Goto strings. We will also talk about an effective action for superconducting cosmic strings.

1.4.1 Nambu-Goto Strings

The Nambu-Goto action reduces the complexity of field theory when studying vortex configurations. It can be deduced from the Abelian-Higgs Lagrangian 1.5 [9], with a change in the coordinates to the string worldsheet ones, which, hereafter, we shall write as σ^0 and σ^1. By considering the lowest order on the fraction between the vortex width and its curvature radius, we are left with the action

$$S = \mu_0 \int \sqrt{-\gamma} d^2\sigma, \tag{1.10}$$

where the string tension μ_0 results from the perpendicular space integration and has units of energy squared. The area element is given by $d^2\sigma = d\sigma^0 d\sigma^1$ and γ is the determinant of the worldsheet metric γ_{ab}, which has the form

$$\gamma_{ab} = g_{\mu\nu} dx^\mu_{,a} dx^\nu_{,b}. \tag{1.11}$$

Here, and throughout the rest of this thesis, greek indices will refer to spacetime coordinates,

latin letters from the middle of the alphabet to space coordinates and letters from the beginning (like the ones in the previous equation) to the string worldsheet coordinates.

These are the Nambu-Goto strings and are the most simple vortex configurations, with no features other than spacetime dynamics. Therefore, if we want to study current-carrying strings, as we do, we need to find an effective action that allows for extra degrees of freedom.

1.4.2 Effective Action for Superconducting Strings

In the case of superconducting strings, integrating over the perpendicular degrees of freedom can be a little bit trickier. Several considerations are taken into account, as it is explained in more detail in [6, 10]. First of all, the current should be a lot smaller than the critical one (there is a value above which the current starts lurking, leading to energy losses), and the potential vector A_μ should not vary substantially across the string width.

Other thing taken into consideration, when arriving to an effective action for superconducting strings, is that, in two dimensions, a conserved current can always be written as a derivative of a scalar field, φ. The full deduction can be seen in [6]. Jumping to the final form of the action, we have

$$S = -\mu_0 \int \left\{ \sqrt{-\gamma} - \frac{1}{2}\sqrt{-\gamma}\gamma^{ab}\varphi_{,a}\varphi_{,b} + eA_\mu x^\mu_{,a}\varepsilon^{ab}\varphi_{,b} \right\} d^2\sigma, \tag{1.12}$$

The scalar field is only defined in the string and can be seen as the degree of freedom embedded on the complex phase θ of subsection 1.3. The usual ε^{ab} is the Levi-Civita tensor, with $\varepsilon^{01} = 1$.

The first term in Equation 1.12 is the familiar Nambu-Goto expression. The second one describes the worldsheet current within the string, and the last one is the current coupling to the electromagnetic gauge potential. It should be noticed that the usual electromagnetic term, proportional to $|F|^2$ was omitted.

There was also a change of units, in relation to [10], in order to write a dimensionless Lagrangian inside of the integral in Equation 1.12. That was possible through the following transformations

$$\varphi = \frac{\varphi^*}{\sqrt{\mu_0}}, \qquad e = \frac{e^*}{\sqrt{\mu_0}}, \tag{1.13}$$

where * denotes the entities used in the previous work already mentioned. Further ahead, I'll be using this action to study the evolution of a string network in the presence of an external magnetic field.

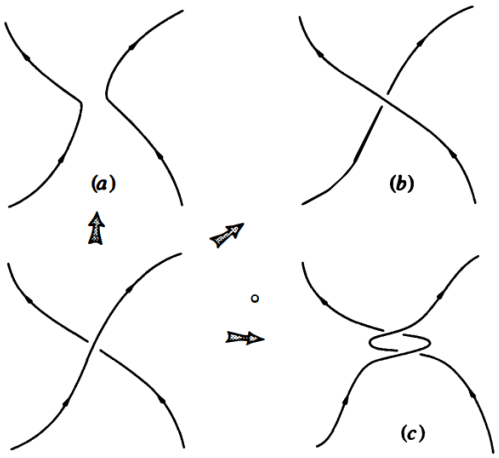


Figure 1.1: When strings intersect they can: a) reconnect, b) not interact at all and c) entangle [10]

1.5 Loop formation

In the beginning, knowing how topological defects in cosmic scales would evolve was of major importance. In fact, it was thought that cosmic strings could be behind the generation of density fluctuations, which would give birth to the galaxies we see today. Later, the Cosmic Microwave Radiation measurements strongly backed the inflation and threw the topological defects to the backstage. This put severe restrictions on cosmic strings, as they could no longer dominate the energy content of the Universe. This was a possibility for their evolution. Another, which was also considered as an attractor, was the scaling regime, where the strings length would scale as the cosmological time [11]. For that to happen, strings would have to lose energy. The main energy loss mechanism was the production of loops. These loops would then decay via gravitational radiation [12] or particle production (for current carrying strings, electromagnetic radiation would dominate the decaying process).

Loop formation happens when two segments of string cross each other. The interaction between them will depend on the string field theory model considered, as the one-dimensional approach is no longer a good approximation. There is a certain probability of the strings to not interact at all - specially if they were formed in symmetry breaking phase transitions at different energy scales. However, if that's not the case, its much more probable for them to interact and exchange partners.

Figure 1.1 represents the possible outcomes when strings intersect with each other. Entanglement is a more complex situation, but can also happen. Besides the radiation emitted by the loops, the kinks and cusps formed during the production of loops, are also a main contributor of energy losses [13, 14].

2 Cosmic String Evolution

In this chapter, I will describe, in more detail, how the cosmic string network evolves through time. As I do that, I shall highlight what are the dominant processes driving their evolution as well as possible energy loss mechanisms.

I'll start by introducing VOS, which treats the string network as a thermodynamic system, and characterizes it through macroscopic quantities, specifically, the correlation length and the root mean square (rms) velocity. This model describes the evolution of the featureless Nambu-Goto strings. I'll then present an extension of VOS model which tackles current-carrying strings.

2.1 VOS

The VOS model, studied in detail in [15–17], considers the evolution of the string network in the context of an expanding Universe. As it was said before, cosmic strings relevance for the background dynamics in the current best-fit Lambda Cold Dark Matter (ΛCDM) model, is of minimal importance. This is due to the constraints imposed by the Cosmic Microwave Background (CMB), which do not allow the strings to compose a substantial fraction of the Universe's energy. Therefore, backreaction in the metric, due to the cosmic strings, is not considered.

Consequently, strings would evolve in a background metric, $g_{\mu\nu}$, given by the Friedmann–Lemaître–Robertson–Walker (FLRW) metric, $ds^2 = a^2\left(dt^2 - d\mathbf{x}^2\right)$, with a being the scale factor. The strings 2-dimensional surface can be described by worldsheet coordinates, σ^a, and spacetime coordinates, $x^\mu = x^\mu(\sigma^a)$. There are extra degrees of freedom in the choice of these coordinates. To simplify the relation between string evolution and the expansion of the Universe, the first gauge condition that is imposed is identifying the worldsheet time-like coordinate with the conformal time, $\sigma^0 = \tau$. The other coordinate, σ^1, which is space-like, will, from now on, for simplifying purposes, be written as σ. We may yet choose another gauge condition. In the VOS model the velocity of the string is considered to be orthogonal to the string direction, $\dot{x}^\mu x'_\mu = 0$. Here dot and prime derivatives are with respect to conformal time, τ, and the space-like coordinate, σ. Since both coordinate are independent, and having $x^0 = \tau$, the previous gauge conditions simplify to $\dot{\mathbf{x}} \cdot \mathbf{x}' = 0$ (bold characters identify 3-vectors; in this case $x^\mu = (\tau, \mathbf{x})$).

With these choices, the worldsheet metric is given by

$$\gamma_{ab} = \begin{bmatrix} a^2\left(1-\dot{\mathsf{x}}^2\right) & 0 \\ 0 & -a^2\mathsf{x}'^2 \end{bmatrix}, \tag{2.1}$$

where $\dot{\mathsf{x}}^2 = \dot{\mathbf{x}}\cdot\dot{\mathbf{x}}$ and $\mathsf{x}'^2 = \mathbf{x}'\cdot\mathbf{x}'$, as usual. From here, it is straightforward to deduce the determinant, $\gamma = -a^4\left(1-\mathsf{x}^2\right)\mathsf{x}'^2$. The inverse of the metric, γ^{ab}, is similar to γ_{ab}: both diagonal terms are the inverse and the off-diagonal ones are the same.

In order to get a equation of motion for the strings, from the Nambu-Goto action 1.10, we must vary it with respect to the position. The variation of the determinant is given by the well known expression

$$\delta\gamma = \gamma\gamma^{ab}\delta\left(\gamma_{ab}\right). \tag{2.2}$$

We can use Equation 2.1 to vary the worldsheet metric, getting

$$\delta\left(\gamma_{ab}\right) = 2g_{\mu\nu}x^{\nu}_{,b}\left(\delta x^{\mu}\right)_{,a} + x^{\lambda}_{,a}x^{\nu}_{,b}g_{\lambda\nu,\mu}\delta x^{\mu}. \tag{2.3}$$

We will have then two terms inside the integral. The first term can be integrated by parts, so we can take the variation of the position outside of the derivative. Doing that, and considering the principle of least action, we arrive at the equation of motion:

$$\frac{\partial}{\partial\sigma^a}\left[\sqrt{-\gamma}\gamma^{ab}g_{\mu\nu}x^{\nu}_{,b}\right] + \frac{1}{2}\sqrt{-\gamma}\gamma^{ab}x^{\lambda}_{,a}x^{\nu}_{,b}g_{\lambda\nu,\mu} = 0. \tag{2.4}$$

This equation can be unfolded in two, whether μ is a time or spatial index

$$\dot{\epsilon} + 2\frac{\dot{a}}{a}\epsilon\dot{\mathsf{x}}^2 = 0 \tag{2.5}$$

$$\ddot{\mathbf{x}} + 2\frac{\dot{a}}{a}\left(1-\dot{\mathsf{x}}^2\right)\dot{\mathbf{x}} = \frac{1}{\epsilon}\left(\frac{\mathsf{x}'}{\epsilon}\right)', \tag{2.6}$$

where $\epsilon = \sqrt{\frac{\mathsf{x}'^2}{1-\dot{\mathsf{x}}^2}}$. This quantity corresponds to the dimensionless energy per unit length and plays a crucial role in the averaging process and in the extended models as well. Therefore, the first equation tells us how the expansion of the Universe serves as a damping term, leading to energy losses. We should also note that this term is proportional to the velocity squared. So, in the ultra-relativistic regime, the strings lose energy the fastest.

In [17], the authors considered an additional energy loss mechanism. In earlier times, where the Universe was filled with a radiation fluid background, the strings motion would be affected by particle scattering. For global strings, the dominant process would be the Everett scattering,

while for gauge ones, the main contribution comes from Aharanov-Bohm scattering. They successfully added a microscopical term, describing this phenomena.

The macroscopic quantities of the thermodynamical approach, in this model, are the correlation length, L, and the rms velocity, v. Both this quantities are related to the microphysics of the system through the process of averaging. In fact, any quantity $\mathcal{O}$, can be averaged

$$\langle \mathcal{O} \rangle = \frac{\int \mathcal{O} \epsilon d\sigma}{\int \epsilon d\sigma}. \tag{2.7}$$

So, the energy per unit length serves as a weighting function. Regions where the string is moving faster, will have a bigger contribution to the overall value of $\langle \mathcal{O} \rangle$. The rms velocity is then given by $v = \sqrt{\langle \dot{\mathbf{x}}^2 \rangle}$.

The correlation length, on the other hand, has a more phenomenological origin. One assumes the strings to have a Brownian motion. In this case, the energy is given by

$$E = \frac{\mu_0 V}{a^2 L^2}, \tag{2.8}$$

where V is a physical volume and therefore scales as $V \propto a^3$, which means $E \propto aL^{-2}$. It is important to note that this lengthscale is a comoving one. On the other hand, the action 1.10 allows us to compute the energy-momentum tensor. It is with no surprise that the overall energy is given by $E = \mu_0 a \int \epsilon d\sigma$.

Putting together the previous definitions and the averaging of the microscopical equations of motion, we can determine the evolution equations that dictate how the correlation lengthscale and the velocity of the strings evolve in time.

When averaging, we are integrating over the space-like parameter σ, which shall run over the entire string network. This would imply the integration to be made across lengths far superior than the correlation lengthscale. Therefore, when averaging, we are summing the contribution of several, uncorrelated strings with size L. Nevertheless, additional assumptions should be made, as is clear in [18]:

- During the averaging process, the variables (the positive definite ones, mainly) were considered uncorrelated. In a generic form, we would have

$$\langle \mathcal{F}(\mathcal{O}) \rangle \approx \mathcal{F}(\langle \mathcal{O} \rangle) \tag{2.9}$$

  This approximation is backed by numerical simulations [15] evaluating and comparing the value of even powers of the rms velocity (for example, in [10] $\langle \dot{\mathbf{x}}^2 \rangle^2 - \langle \dot{\mathbf{x}}^4 \rangle$ was calculated,

yielding a small difference). This strongly simplifies the equations and has a more pivotal role in the extended models.

- The entire network is assumed to feature periodic boundary conditions. There is a certain intuition for this. It doesn't matter if the correlation length is smaller than the Hubble radius. Strings stretch along the entire network, and if we follow it, we will come back to the same place, because they are loops on bigger scales (it should be mentioned that there are more exotic types of strings, namely strings with loose ends - with monopoles [19] - for which this approximation seems to fail at first sight). Therefore, when integrating a total derivative, we can substitute it by $\int \frac{\partial}{\partial\sigma}\left[\mathcal{F}\left(\mathcal{O}\right)\right]d\sigma \rightarrow \oint \frac{\partial}{\partial\sigma}\left[\mathcal{F}\left(\mathcal{O}\right)\right]d\sigma \approx 0$. This is not exactly 0, because $\mathcal{F}$ may not be continuous if, for example, we are in the presence of cusps and kinks. However, as we are summing through all the strings, it is expected for the positive and negative contributions to compensate each other, yielding a negligible value.

Taking all this into account, the evolution of the lengthscale is given by

$$\frac{dL}{d\tau} = HLv^2, \tag{2.10}$$

where H is the Hubble parameter, $H = \frac{\dot{a}}{a}$. There is a small difference between this equation and the correspondent one in [15], which is due to the fact that, working with the physical lengthscale introduces the term $-HL$ in the L. H. S. of Equation 2.10. On the other hand, the velocity evolves according to

$$\dot{v} = \left(1-v^2\right)\left[\frac{k_v}{R} - 2Hv\right]. \tag{2.11}$$

Equation 2.11 introduces two different parameters. R is the comoving curvature radius and is defined through

$$\frac{\hat{\mathbf{u}}}{R} = \frac{\partial^2\mathbf{x}}{\partial s^2}, \tag{2.12}$$

where s is the physical length along the string, $ds = \sqrt{\mathbf{x}'^2}d\sigma$ and $\hat{\mathbf{u}}$ an unit vector. In the VOS model, R is identified with L, living up to the model designation. On the other hand, k_v is called the momentum parameter and is given by

$$k_v = \frac{\left\langle\left(1-\dot{\mathbf{x}}^2\right)\left(\ddot{\mathbf{x}}\cdot\hat{\mathbf{u}}\right)\right\rangle}{v\left(1-v^2\right)}. \tag{2.13}$$

For a straight line, the unit vector $\hat{\mathbf{u}}$ should align with the velocity vector, and we would

get $k = 1$. However, for a string which is not that smooth, when integrating over the network, it is not expected for the momentum parameter to yield the same value. Consequently, k is sensible to the small-scale structure. In fact, being a phenomenological parameter, its behavior was studied in numerical simulations [16] and an analytical approximation to the best fit was determined

$$k_v = \frac{2\sqrt{2}}{\pi}\left(1-v^2\right)\left(1+2\sqrt{2}v^3\right)\frac{1-8v^6}{1+8v^6}, \tag{2.14}$$

where approximations for the relativistic and non-relativistic regimes can be seen in [16].

2.1.1 Energy Loss Terms

We already saw how the expansion of the Universe acts as a damping source term. However, as has already been mentioned, a key role in the string networks evolution, is played by the formation of loops.

Loops form when the strings interact with themselves, and the right way to analyze their formation rates and how they decay, is through string field theory. Clearly, all of this depends on the model giving rise to the strings, because the field solutions in the normal directions of the vortex are crucial for deducing the cross sections, and therefore, the probabilities for the loop formation.

So, it is evident that the Nambu-Goto action 1.10 does not forecast this type of energy losses. Consequently, this term must be placed by hand. [15] made a deep study about loops formation, providing the now standard term $\frac{\tilde{c}v}{2}$, which should be added to the R. H. S. of equation 2.10 (added because smaller energies correspond to bigger L). The loop chopping efficiency parameter, $\tilde{c}$, is a phenomenological quantity that encompasses the hidden features of loop formation. Again, its value was studied by numerical simulations. For the radiation and matter era the best fit value was $\tilde{c} = 0.23 \pm 0.04$ [16].

2.2 CVOS

In the previous section the VOS model was introduced in detail. As it characterizes Nambu-Goto strings, which are simpler than the one considered in this section, some features that will remain useful were desiccated for a better understanding.

The formalism considered here is CVOS and it first appeared in [18,20], although extensions of the VOS model featuring charge and currents in the chiral limit were already considered before [21–23]. This model proposes to study current carrying strings. Although the effective action 1.12 is already a simple description of superconducting strings, its eloquent aspect hides

the complex dynamics between the scalar field and the gauge potential field. The charge and current in one place of the string will create electromagnetic fields that will affect other regions on the string. In turn, these places have the same effect on the previous patch, which, alongside with the backreaction of the scalar field on the strings dynamics and vice-versa, makes an analytical analysis almost impossible.

The CVOS presents a nice way to prevent these situations. Instead of dealing with the effective action for superconducting strings, it extends the previous Nambu-Goto one, in order to allow for an extra degree of freedom. The proposed action is the following

$$S = -\mu_0 \int \sqrt{-\gamma} f\left(\mathsf{k}\right) d^2\sigma, \tag{2.15}$$

where $\mathsf{k} = \gamma^{ab}\varphi_{,a}\varphi_{,b}$ is the chirality parameter. It is an invariant scalar, the same no matter the reference frame. It measures whether the current is time-like, $\mathsf{k} > 0$, space-like, $\mathsf{k} < 0$ or light-like, $\mathsf{k} = 0$, in which cases, we say we are in the electric, magnetic or in the chiral regime, respectively. On the other hand, $f\left(\mathsf{k}\right)$ is a function that tries to describe the microphysical behavior of superconducting cosmic strings.

Considering the worldsheet metric given by Equation 2.1, the chirality parameter becomes

$$\mathsf{k} = \frac{\dot{\varphi}^2}{a^2\left(1 - \dot{\mathsf{x}}^2\right)} - \frac{\varphi'^2}{a^2\mathsf{x}'^2} \equiv q^2 - j^2, \tag{2.16}$$

where in the last equality, the worldsheet charge, q, and current, j, were defined.

The energy-momentum tensor in the string can be obtained by varying the action with respect to the background metric. To represent it in a more organized way, we can use the orthogonal unit vectors $\tilde{u}^\mu = \frac{\sqrt{\epsilon}\dot{x}^\mu}{\sqrt[4]{-\gamma}}$ and $\tilde{v}^\mu = \frac{x'^\mu}{\sqrt{\epsilon}\sqrt[4]{-\gamma}}$. They are time-like and space-like, respectively. In these coordinates we have

$$T^{\mu\nu}\left(y\right) = \frac{\mu_0}{\sqrt{-g}} \int \delta^{(4)}\left(y - x\left(\sigma\right)\right) \sqrt{-\gamma} \left[\tilde{U}\tilde{u}^\mu\tilde{u}^\nu - \tilde{T}\tilde{v}^\mu\tilde{v}^\nu + \Phi\left(\tilde{u}^\mu\tilde{u}^\nu + \tilde{v}^\mu\tilde{v}^\nu\right)\right] \tag{2.17}$$

where the dimensionless parameters are given by $\tilde{U} = f - 2\frac{df}{d\mathsf{k}}q^2$, $\tilde{T} = f - 2\frac{df}{d\mathsf{k}}j^2$ and $\Phi = -2qj\frac{df}{d\mathsf{k}}$. $\delta^{(4)}$ is the four dimensional Dirac delta, and it assures that we remain on the string. Using the energy-momentum tensor to calculate the overall energy content, we get $E = \mu_0 a \int \tilde{U}\epsilon d\sigma$. Therefore, $\tilde{U}$ can be seen as the dimensionless energy density in the string. In the same way, $\tilde{T}$ is related with the string tension.

Acting in the same way in order to determine the equations of motion, we arrive at

$$\frac{\partial}{\partial\tau}\left(\epsilon\tilde{U}\right)+\frac{\dot{a}}{a}\epsilon\left[\left(\tilde{U}+\tilde{T}\right)\dot{\mathsf{x}}^2+\tilde{U}-\tilde{T}\right]=\frac{\partial\Phi}{\partial\sigma}, \tag{2.18}$$

$$\epsilon\tilde{U}\ddot{\mathbf{x}}+\frac{\dot{a}}{a}\epsilon\left(\tilde{U}+\tilde{T}\right)\left(1-\dot{\mathsf{x}}^2\right)\dot{\mathbf{x}}=\frac{\partial}{\partial\sigma}\left(\frac{\tilde{T}}{\epsilon}\mathbf{x}'\right)+\left(2\frac{\dot{a}}{a}\Phi+\dot{\Phi}\right)\mathbf{x}'+2\Phi\dot{\mathbf{x}}'. \tag{2.19}$$

If, instead of the positions, we vary φ, we get the field equation describing its evolution

$$\frac{\partial}{\partial\tau}\left[a\frac{df}{d\mathsf{k}}\sqrt{q^2\mathsf{x}'^2}\right]=\frac{\partial}{\partial\sigma}\left[a\frac{df}{d\mathsf{k}}\sqrt{j^2\left(1-\dot{\mathsf{x}}^2\right)}\right]. \tag{2.20}$$

There is a small caveat to all of these equations. We only have four variables, **x** and φ, for five equations. Well, the equations are not written in terms of the scalar field, but of the charge and current instead. However, if we take these two to be our variables, there is one more equation which results from the following redundancy on the definition of q and j: $\frac{\partial^2\varphi}{\partial\tau\partial\sigma}=\frac{\partial^2\varphi}{\partial\sigma\partial\tau}$ - that is, somehow the time derivative of the current is related with the spatial derivative of the charge. The equation reads

$$q'=\epsilon\dot{j}+\left[\frac{\dot{a}}{a}-\frac{\mathbf{x}''\cdot\dot{\mathbf{x}}}{\mathsf{x}'^2}\right]\epsilon j+\frac{\dot{\mathbf{x}}\cdot\dot{\mathbf{x}}'}{1-\dot{\mathsf{x}}^2}q. \tag{2.21}$$

And so, there seems to be always one more equation. However, as expected, only four of the six previous equations in 2.18, 2.19, 2.20, 2.21 are linearly independent. If we unfold Equation 2.19 by projecting them along the string and velocity directions, we arrive at two linearly independent equations. However, again, substituting Equation 2.18 and 2.20 into the one along the string direction would yield the triviality $0=0$.

Therefore, one of the equations between Equation 2.18, Equation 2.20 and Equation 2.21 alongside with

$$\tilde{U}\frac{\partial}{\partial\tau}\left(\dot{\mathsf{x}}^2\right)+2\left[\frac{\dot{a}}{a}\left(\tilde{U}+\tilde{T}\right)\dot{\mathsf{x}}^2-\tilde{T}\frac{\mathbf{x}''\cdot\dot{\mathbf{x}}}{\mathsf{x}'^2}-2\frac{\Phi}{\epsilon}\frac{\dot{\mathbf{x}}\cdot\dot{\mathbf{x}}'}{1-\dot{\mathsf{x}}^2}\right]\left(1-\dot{\mathsf{x}}^2\right)=0, \tag{2.22}$$

which results from the scalar product of equation 2.19 with $\dot{\mathbf{x}}$, form a set of linearly independent equations that govern the system evolution. Now, it seems we have to few equations. However, we should remind ourselves that the gauge condition $\mathbf{x}'\cdot\dot{\mathbf{x}}=0$ reduces the number of free variables.

Before extracting the macroscopic equations, we shall introduce the new macroscopic quantities. This model considers a scalar field living in the string and contributing, as it is clear in the equations above, to the string dynamics. We have already seen that this field contributes to the overall energy of the network, through $\tilde{U}$. Therefore, considering again a Brownian motion,

the characteristic lengthscale, L, has now a different but analogous definition. This lengthscale is associated with the energy both on the strings themselves and on charges and currents. However, we can also consider only the energy on the strings, given by the VOS expression. To this quantity we shall call the bare energy, E_0, and associate the correlation lengthscale, ξ. This measures the average distance above which the strings are uncorrelated. The Brownian assumption allows for the following definitions: $E \equiv \frac{\mu_0 V}{a^2 L^2}$ and $E_0 = \frac{\mu_0 V}{a^2 \xi^2}$. We can relate the two through

$$\frac{E}{E_0} = \frac{\xi^2}{L^2} = \frac{\int \tilde{U} \epsilon d\sigma}{\int \epsilon d\sigma} \equiv \langle \tilde{U} \rangle. \tag{2.23}$$

The total energy is always greater or equal to the bare string energy. This means that $\xi \geq L$, all the time. We can see that their fraction depends only on the microphysics present on f and which manifests itself through the bigger scales. So, instead of being a one-scale model, we have two lengthscales. We could have three, however the comoving curvature radius, which already appeared before, is identified with the correlation length, $R \to \xi$.

Besides this new addition, CVOS takes into consideration the macroscopic counterpart of the charge and current as well. They will be designated by Q and J, respectively. And their definition is straightforward, $Q^2 = \langle q^2 \rangle$ and $J^2 = \langle j^2 \rangle$. By considering the previous assumption of uncorrelated variables, while averaging, we can see that the fraction of the bare and total energy, depends only on the macroscopic charge and current. The average equations resulting from the previous analysis are

$$\dot{L} = \frac{\dot{a}}{a} \frac{L}{F - 2Q^2 F'} \left\{ \left[F - \left(Q^2 - J^2 \right) F' \right] v^2 - \left(Q^2 + J^2 \right) F' \right\} \tag{2.24a}$$

$$\dot{v} = \frac{1 - v^2}{F - 2Q^2 F'} \left\{ \frac{k_v}{\xi} \left(F + 2J^2 F' \right) - 2v \frac{\dot{a}}{a} \left[F - \left(Q^2 - J^2 \right) F' \right] \right\} \tag{2.24b}$$

$$\frac{dJ^2}{d\tau} = 2J^2 \left[\frac{v k_v}{\xi} - \frac{\dot{a}}{a} \right] \tag{2.24c}$$

$$\frac{dQ^2}{d\tau} = 2Q^2 \frac{F' + 2J^2 F''}{F' + 2Q^2 F''} \left[\frac{v k_v}{\xi} - \frac{\dot{a}}{a} \right], \tag{2.24d}$$

where $F \equiv \langle f \rangle$, $F' \equiv \left\langle \frac{df}{d\mathsf{k}} \right\rangle$ and $F'' \equiv \left\langle \frac{d^2 f}{d\mathsf{k}^2} \right\rangle$. Here the primes denote higher derivative orders on the averaging function, and should not be confused with derivatives with respect to σ (in fact, all this quantities, once they are the byproduct of the integration along σ, i. e., along the string network, do not depend on it). The previously mentioned correspondence, $R = \xi$, is also evident.

We can also add another equation for the evolution of the correlation length. However, it

would only make the problem seem more complex than it truly is. In fact, knowing the evolution of L, Q and J, alongside with Equation 2.23, allows us to determine ξ directly. We may introduce the quantity $W = \sqrt{F - 2Q^2F'}$, which will alleviate the notation, and we have $\xi = WL$.

Again, we need to add the energy loss terms phenomenologically. Proceeding as previously, we can add the loop formation term as

$$\frac{\dot{\xi}}{\xi} = \left(\frac{\dot{\xi}}{\xi}\right)_0 + \frac{\tilde{c}}{2}\frac{v}{\xi}, \tag{2.25}$$

where the index 0 denotes the parameter evolution before considering energy loss mechanisms. A similar term should appear in the characteristic lengthscale equation

$$\frac{\dot{L}}{L} = \left(\frac{\dot{L}}{L}\right)_0 + g\left(Q, J\right)\frac{\tilde{c}}{2}\frac{v}{\xi}. \tag{2.26}$$

The function $g\left(Q, J\right)$ describes how regions with different charges and currents are more or less prone to form loops. These two equations will also affect the evolution of the charge and current, because L and ξ are related through W, which, in turn, depends on Q and J.

The final form of the macroscopic CVOS equations is

$$\dot{L} = \frac{\dot{a}}{a}\frac{L}{W^2}\left\{\left[W^2 + \left(Q^2 + J^2\right)F'\right]v^2 - \left(Q^2 + J^2\right)F'\right\} + g\frac{\tilde{c}}{2}\frac{v}{W} \tag{2.27a}$$

$$\dot{v} = \frac{1 - v^2}{W^2}\left\{\frac{k_v}{\xi}\left[W^2 - 2\left(Q^2 + J^2\right)F'\right] - 2v\frac{\dot{a}}{a}\left[W^2 + \left(Q^2 + J^2\right)F'\right]\right\} \tag{2.27b}$$

$$\frac{dJ^2}{d\tau} = 2J^2\left[\frac{vk_v}{\xi} - \frac{\dot{a}}{a}\right] + \rho\tilde{c}\frac{v}{L}\frac{(g-1)W}{F' - 2Q^2F''} \tag{2.27c}$$

$$\frac{dQ^2}{d\tau} = 2Q^2\frac{F' + 2J^2F''}{F' + 2Q^2F''}\left[\frac{vk_v}{\xi} - \frac{\dot{a}}{a}\right] + (1-\rho)\,\tilde{c}\frac{v}{L}\frac{(g-1)W}{F' + 2Q^2F''}, \tag{2.27d}$$

where F was everywhere substituted by W and ρ is a bias parameter measuring whether regions with more charge than current, or vice-versa, are more prone to form loops. The case where there is no bias happens for $\rho = 0.5$. Regions with greater current dominate the energy loss contribution if $\rho \to 1$ and the opposite if $\rho \to 0$.

The reason why we substituted F for W was for the notation to not become very cumbersome (more than it already is). It will also help us track some quantities when we search for scaling solutions.

3 Circular Loops

In this chapter, I'll delve in the evolution of loops. In subsection 1.5 we saw how these entities may form and their fate. In principle, they decay via gravitational waves [24], or, if they detach from superconducting strings, via electromagnetic radiation [25].

However, in the last case, the fate of the loops may not be that straightforward. In fact, the extra degree of freedom can play a crucial role in stabilizing the loop. In simple words, the additional angular momentum of the scalar field may prevent the loop from disappearing. I'll analyze this possibility through the microscopic equations of the CVOS.

3.1 Loop Configuration and Microscopic Equations

The evolution of loops was studied in [12], where the author proposed a way to configure the loop's shape through two simple numbers. However, here I'll study the simplest of loop configuration: a circle. Although this may not seem very realistic, the tension will try to straighten out the loop, leading to a more smooth configuration, with the limiting case corresponding to a circle.

And so, our loop will be parameterized by $\mathbf{x} = r(\tau)(\cos\theta, \sin\theta, 0)$, where it was assumed to lie in the xy plane, with no loss of generality. The radius of the loop is given by r and only depends on the conformal time. If we would allow it to vary with θ, which is the common angular parameter that parameterize the ring, we would soon not have a circle.

Noticing that the prime derivatives are now relative to this parameter θ, and realizing that $\hat{e}_r \equiv (\cos\theta, \sin\theta, 0)$, $\hat{e}'_r = \hat{e}_\theta \equiv (-\sin\theta, \cos\theta, 0)$ and $\hat{e}''_r = -\hat{e}_r$, we may write: $\dot{\mathbf{x}} = \dot{r}\hat{e}_r$, $\ddot{\mathbf{x}} = \ddot{r}\hat{e}_r$, $\mathbf{x}' = r\hat{e}_\theta$ and $\mathbf{x}'' = -r\hat{e}_r$. This is in accordance with our previous gauge conditions, because the unit vectors $\hat{e}_r$ and $\hat{e}_\theta$ are orthogonal, and therefore $\dot{\mathbf{x}} \cdot \mathbf{x}' = 0$. It also allows us to simplify the following relevant expressions

$$\frac{\dot{\mathbf{x}}' \cdot \mathbf{x}'}{\mathrm{x}'^2} = \frac{\dot{r}}{r} \quad \text{and} \quad \frac{\dot{\mathbf{x}}' \cdot \dot{\mathbf{x}}}{1 - \dot{\mathbf{x}}^2} = 0. \tag{3.1}$$

Another important quantity is the dimensionless bare string energy density, $\epsilon = \sqrt{\frac{r^2}{1-\dot{r}^2}}$. In these coordinates, Equation 2.22 becomes

$$\ddot{r} = -\left[\frac{\dot{a}}{a}\dot{r}\left(1 + c_T^2\right) + \frac{c_T^2}{r}\right]\left(1 - \dot{\mathrm{x}}^2\right), \tag{3.2}$$

where $c_T^2 \equiv \frac{\tilde{T}}{\tilde{U}}$ is the velocity of transversal perturbations within the string, and should be greater than 0 and smaller than unity.

Regarding the charge, q, and current, j, the circle configuration does not impose anything, and therefore, we have $q = q(\tau, \theta)$ and $j = j(\tau, \theta)$. However, Equation 3.2 is a time-dependent equation, only. Consequently, c_T^2, which depends on q and j, must be uniform along the loop. This restriction creates a relation between the charge and current values.

For simplifying purposes, we will consider a uniform charge and current, and the condition $\frac{\partial c_T^2}{\partial \theta} = 0$ is immediately satisfied. The equations that will rule the evolution of charge and current within the ring may be found by rewriting Equation 2.20 and Equation 2.21

$$\frac{dj}{d\tau} = -\left[\frac{\dot{a}}{a} + \frac{\dot{r}}{r}\right] j \tag{3.3}$$

$$\frac{dq}{d\tau} = -\frac{\frac{df}{d\mathsf{k}} + 2j^2\frac{d^2f}{d\mathsf{k}^2}}{\frac{df}{d\mathsf{k}} + 2q^2\frac{d^2f}{d\mathsf{k}^2}}\left[\frac{\dot{a}}{a} + \frac{\dot{r}}{r}\right] q. \tag{3.4}$$

These are very simple equations and we can see that both charge and current time derivatives are proportional to themselves. This means that, if one has a vanishing initial value, it will remain that way. We will later see that describing the system as a function of q and j is not the most efficient way. So we will change variables $q,\, j \to \mathsf{k},\, y$, where $\mathsf{k} \equiv q^2 - j^2$ is the chirality and $y \equiv q^2 + j^2$ shall be called the total charge. In terms of these quantities we have

$$\dot{y} = -A\left[(B+1)\, y + (B-1)\, \mathsf{k}\right] \tag{3.5}$$

$$\dot{\mathsf{k}} = -A\left[(B-1)\, y + (B+1)\, \mathsf{k}\right], \tag{3.6}$$

where $A = \frac{\dot{a}}{a} + \frac{\dot{r}}{r}$ and $B = \frac{\frac{df}{d\mathsf{k}} + 2j^2\frac{d^2f}{d\mathsf{k}^2}}{\frac{df}{d\mathsf{k}} + 2q^2\frac{d^2f}{d\mathsf{k}^2}}$.

One feature that was not visible with the previous variables is that, if $\mathsf{k} = 0$, then its derivative also vanishes. This happens because, in that case, $B = 1$, and therefore, $\dot{\mathsf{k}} = 0$

As it was said, the purpose here is to study the evolution of these quantities. However the previous equations are written in terms of the unknown function f, which describes the microscopic physics happening within the strings. Therefore, we will consider three models and analyze how the loops evolve on each specific context.

- The linear model is the simplest one. It reads $f(\mathsf{k}) = 1 - \frac{1}{2}\mathsf{k}$ and it is expected to describe current-carrying strings for small charges and currents.

  If we substitute this, we can see that chirality completely disappears from the system equations. That is a particular feature of the linear model and allows for a more analytical study. In fact, we have $c_T^2 = \frac{2-y}{2+y}$ and $B = 1$ (because the second derivative vanishes).

And, from Equation 3.5, we are left with $\dot{y} = -2Ay$. In order for the ring to be stable, we must have $0 < y < 2$.

- The Kaluza-Klein model reads

$$f(\mathsf{k}) = \sqrt{1-\mathsf{k}}. \tag{3.7}$$

This expression was already studied in the literature to characterize the dual model for superconducting strings [26] and wiggly strings [27]. Within this model, both the total charge and chirality are relevant and we have

$$c_T^2 = \frac{2-\mathsf{k}-y}{2-\mathsf{k}+y} \quad \text{and} \quad B = \frac{1+\mathsf{k}-2y}{1-3\mathsf{k}-2y}. \tag{3.8}$$

Again, stable loops require $0 < y < 2-\mathsf{k}$.

- The last model we will study is the Witten one and it is given by

$$f(\mathsf{k}) = \begin{cases} 1-\frac{1}{2}\frac{\mathsf{k}}{1-\alpha\mathsf{k}}, & \text{if } \mathsf{k} \leq 0 \\ 1+\frac{\ln(1-\alpha\mathsf{k})}{2\alpha}, & \text{if } \mathsf{k} > 0 \end{cases} \tag{3.9}$$

It has the peculiarity of having different chirality dependency whether we are in the magnetic, $\mathsf{k} < 0$, or in the electric, $\mathsf{k} > 0$, regime. It results from an analytical approximation to numerical simulations considering the Witten model for superconducting strings [28]. It also introduces a dimensionless parameter, $\alpha = \left(\frac{m_\sigma}{m_H}\right)^2$, where m_σ is the vacuum mass of the current-generating condensate and m_H that of the string-forming Higgs field. According to [28] it must be greater than unity. And thus, we have

$$c_T^2 = \begin{cases} \frac{2-4\alpha\mathsf{k}+(2\alpha+1)\alpha\mathsf{k}^2-y}{2-4\alpha\mathsf{k}+(2\alpha+1)\alpha\mathsf{k}^2+y}, & \text{if } \mathsf{k} \leq 0 \\ \\ \frac{2\alpha(1-\alpha\mathsf{k})+\alpha\mathsf{k}+(1-\alpha\mathsf{k})\ln(1-\alpha\mathsf{k})-2\alpha y}{2\alpha(1-\alpha\mathsf{k})+\alpha\mathsf{k}+(1-\alpha\mathsf{k})\ln(1-\alpha\mathsf{k})+2\alpha y}, & \text{if } \mathsf{k} > 0 \end{cases} \tag{3.10}$$

and

$$B = \begin{cases} \frac{1+\alpha\mathsf{k}-2\alpha y}{1-3\alpha\mathsf{k}-2\alpha y}, & \text{if } \mathsf{k} \leq 0 \\ \frac{1-\alpha y}{1-2\alpha\mathsf{k}-\alpha y}, & \text{if } \mathsf{k} > 0 \end{cases} \tag{3.11}$$

Considering the magnetic regime, we must have $y < 2-4\alpha\mathsf{k}+(2\alpha+1)\alpha\mathsf{k}$. In the electric one, $y < 1-\alpha\mathsf{k}+\frac{1}{2}\mathsf{k}+\frac{1-\alpha\mathsf{k}}{2\alpha}\ln(1-\alpha\mathsf{k})$.

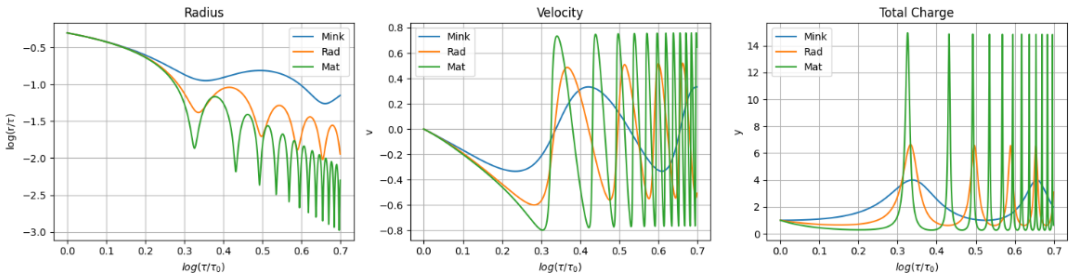


Figure 3.1: From left to right: the first plot represents the radius of the loop in units of conformal time, as function of τ for the different expansion rates. The second and third plots represent the velocity $\dot{r}$ and the total charge y as a function of τ. Blue, orange and green lines correspond to $\lambda = 0$, $\lambda = 1$ and $\lambda = 2$, respectively.

All models coincide in the chiral regime, where k $= 0$, and up to first order.

3.2 Loop Evolution

In this section, we shall solve the previous Equation 3.2 and Equation 3.6 numerically, for the three models. We will also consider three different expansion rates, $\lambda = 0, 1, 2$, corresponding to a Minkowski space-time and the radiation and matter era, respectively (where the scale factor evolves as $a \propto \tau^{\lambda}$). We will begin by analyzing the simpler behavior of the linear model. Then, as our understanding deepens, we will examine the differences between the magnetic and electric regimes in the other models.

3.2.1 The Linear Model

As already mentioned, for the linear model chirality is of no importance. So it doesn't matter its value, the result is always the same, provided the total charge has not changed.

We shall see that the loop's evolution will depend mainly on the initial conditions, such as the initial radius, velocity and total charge. When considering an expanding Universe, the system loses the time translation symmetry, and so, varying the initial time will also influence the evolution of the loops. We can see this if we look closer to the Hubble damping term, $\frac{\dot{a}}{a} = \frac{\lambda}{\tau}$. For $\lambda = 0$ this term vanishes. However, in the radiation or in the matter era, the smaller the times considered, the greater is the damping term (and more difficult it is for the loop to survive).

If we consider a Nambu-Goto ring, i. e., in the limit $y \to 0$, the loop decays. The main features of a circular loop with an initial total charge $y_0 = 1$ are represented in Figure 3.1. The quantity $log\left(\frac{r}{\tau}\right)$ gives us an idea of the loop's size in relation to the horizon. There are several things happening. The most relevant one is that instead of decaying, the loop starts oscillating. We can also see that the ring gains immediately a non-zero velocity and is highly relativistic. The peaks on the total charge correspond to minima in the radius.

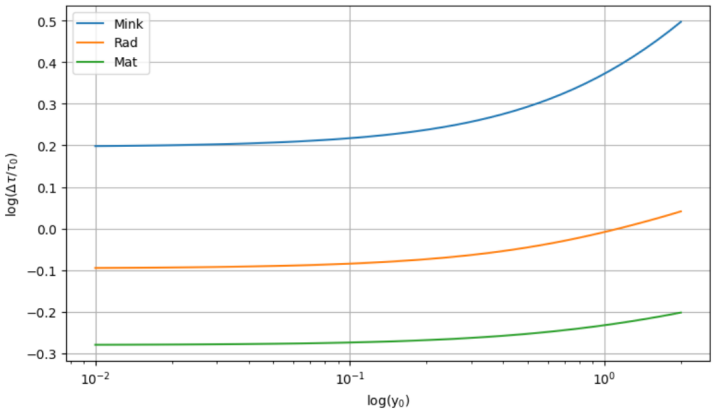


Figure 3.2: The time needed to complete one oscillation after the radius reaches the first minimum. Blue, orange and green lines correspond to $\lambda = 0$, $\lambda = 1$ and $\lambda = 2$, respectively.

There is also a clear difference between the various expansion rates. In Minkowski spacetime the oscillations are longer and the loop's radius is greater when it reaches a minimum. All this points to a greater stability. The opposite happens in the matter era. The oscillations are faster and the radius decreases significantly. The velocity profile consolidates the argument. The high variability of the matter era loop's velocity could lead to instabilities and, in a more realistic case, lead to enormous electromagnetic radiation.

The total charge plot also highlights those differences. The peaks on the matter era loops are way bigger, because a greater charge is needed in order to prevent the loop from disappearing. Again, in more realistic cases, this high value of the charge could lead to charge leaks, leading to energy losses and perhaps to a vanishing loop. Although the total charge reaches values which lead to a negative c_T^2, the integration was not stopped because they probably are a consequence of the lack of microscopic loss terms. Consequently, subsequent results must be carefully interpreted.

The premise that led to this study was that sufficiently charged loops could survive through time (not indefinitely, but at least through a big portion of the Universe's lifetime). So, what happens when we vary the initial total charge? The answer is given in Figure 3.2. There it is represented the time upon which the radius completes one oscillation after reaching its first minimum. It is a measure of the stability of the loop. If we imagine no charge at all, the Hubble damping term and the tension in the string would lead to the continuous decreasing of the loop radius. However, if we increase the charge, the additional angular momentum is expected to delay the radius decreasing, meaning a more stable configuration. That is exactly what happens in Figure 3.2.

We can also see that Minkowski space oscillations are always longer. Therefore, although the initial total charge impacts the time taken in the first oscillation (specially for bigger values),

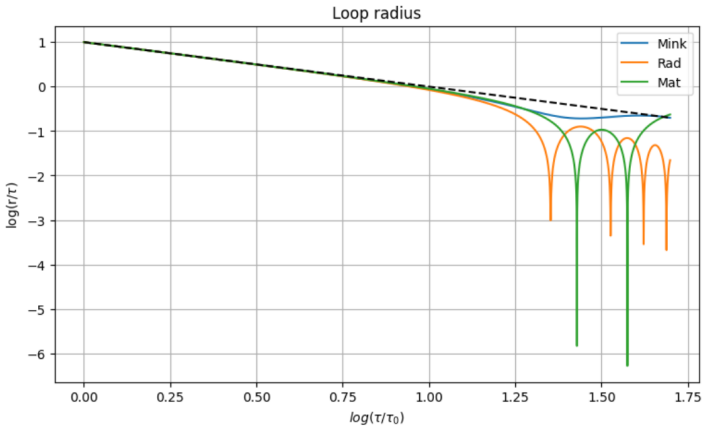


Figure 3.3: Radius of the loop as a function of time. The dashed black line corresponds to a ring with constant radius r_0. Blue, orange and green lines correspond to $\lambda = 0$, $\lambda = 1$ and $\lambda = 2$, respectively.

the expansion rate difference dominates. We should also note that it's easier for the initial charge increase to influence the oscillation for lower expansion rates.

It is also useful to see the difference between loops greater and smaller than the horizon. We can do that by increasing the initial radius to a value of $log\left(\frac{r_0}{\tau_0}\right) = 1$, meaning a size ten times bigger than the horizon. This loop evolution is represented in Figure 3.3.

We can imagine the initial state of this loop. It is so big that different patches are not causally connected. Therefore, if one part starts shrinking, there is not enough time to warn the opposite side to shrink as well. Consequently, we expected the ring to be frozen until it reaches the horizon and that's exactly what happens. The dashed black line in Figure 3.3 represents the radius of a frozen loop with the same initial size. And it is clearly visible that the different loops start to differentiate from $log\left(\frac{r}{\tau}\right) = 0$. The steepness on the velocity values when considering an expanding Universe is also very noticeable. This happens because the total charge had been decreasing since the beginning due to the Hubble damping. And so, it evolves almost as a loop without current.

3.2.2 Kaluza-Klein vs Witten Models

In this subsection, I'll examine the evolution of the loops considering the Kaluza-Klein and the Witten models. In these cases, chirality plays an equally relevant role when compared to the total charge. I'll give a special emphasis to the magnetic and the electric regime. In an approximated way, the chiral regime was already studied, because we can imagine the examined linear loops to be chiral (in the linear model the value of k does not matter; but if we assume k $= 0$, then for reasons already mentioned, we would remain in the chiral regime). On the other hand, all models coincide up to first order. Therefore, the loops studied in the previous subsection correspond to the k $\to 0$ limit of the loops that will be studied here.

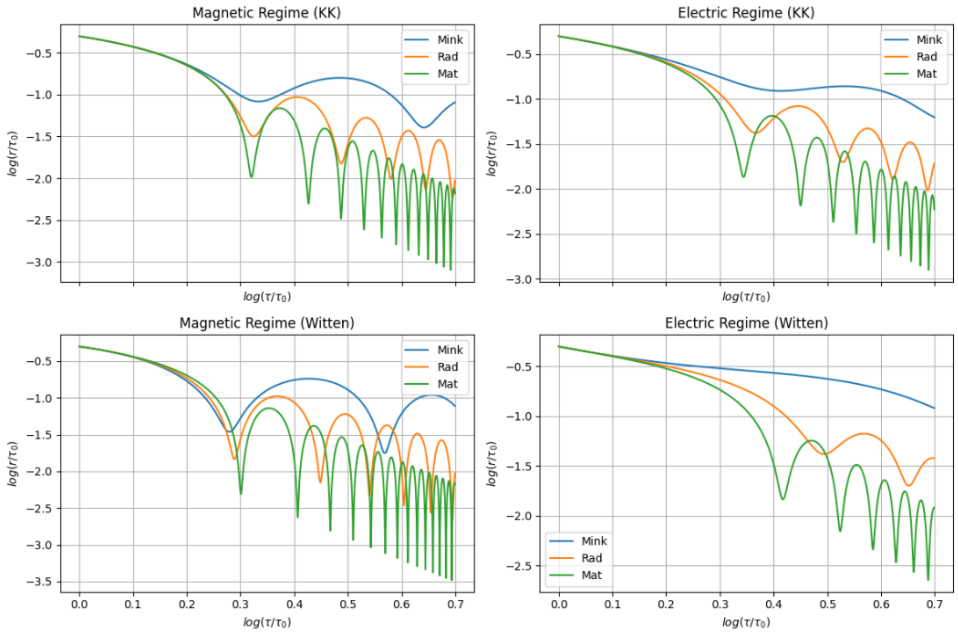


Figure 3.4: Radius of the loop as a function of time. Magnetic and electric regimes are represented on the left and right sides, respectively. The ones above correspond to the Kaluza-Klein model and below to the Witten one. Blue, orange and green lines correspond to $\lambda = 0$, $\lambda = 1$ and $\lambda = 2$, respectively.

In order to analyze the differences between both the magnetic and the electric regimes we determined the evolution of the loop for both models considering the initial chiralities $k_0 = \pm 0.5$. We also considered $\alpha = 1.5$. Figure 3.4 represents the radius of the ring in these four situations.

If we first compare both regimes and remember the previous argument stating that wider oscillations mean more stable loops, then we can assert the electric regime to be a better environment for the stability of loops.

If we now compare both models, the differences change whether we are in the magnetic or in the electric regime. In fact, the magnetic Kaluza-Klein seems to be more stable than the homologous Witten loops. However, the opposite happens in the electric regime. This is mainly due to the different expressions in the Witten dimensionless Lagrangian, whether k is positive or negative.

The total charge profile is straightforward taking into account the analysis made in the linear model. We expect y to rise when the radius reaches a minimum and the peaks to be greater for sharper velocity variations (which correspond to the less stable environments).

Although the total charge behavior is quite predictable, that of chirality needs a little bit more inspection. Figure 3.5 represents the evolution of the loop's chirality for the same four cases.

The first thing we notice is that the sign of k remains the same, so chirality seems to be preserved. In order to have a better understanding of these plots, one should bear in mind that $|k| \leq y$, a consequence of the way they are defined. So, we can regard the absolute value of

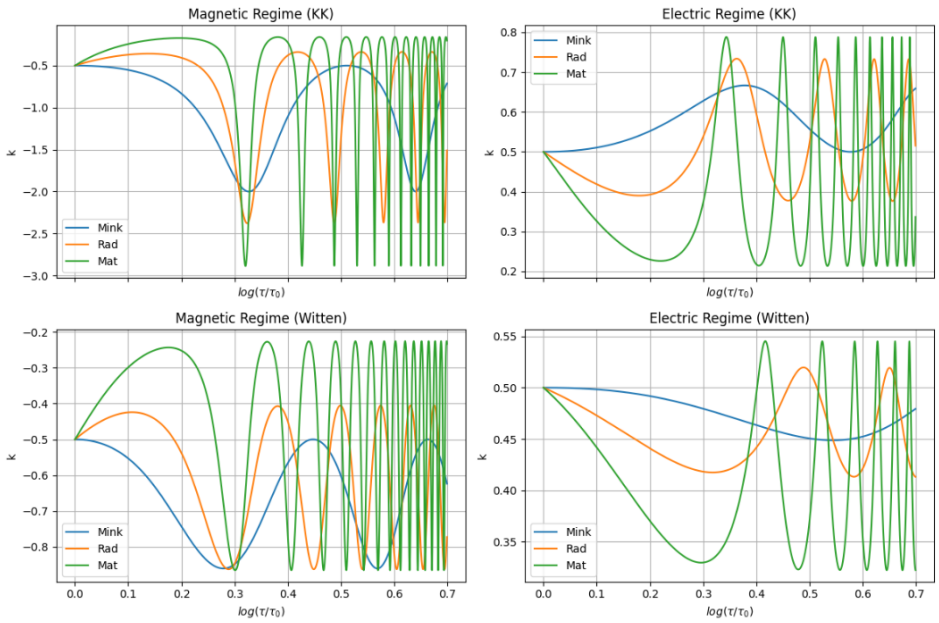


Figure 3.5: Chirality as a function of time. Magnetic and electric regimes are represented on the left and right sides, respectively. The ones above correspond to the Kaluza-Klein model and below to the Witten one. Blue, orange and green lines correspond to $\lambda = 0$, $\lambda = 1$ and $\lambda = 2$, respectively.

chirality as the minimum allowed for the total charge. Although in Figure 3.5 chirality seems to oscillate, in truth it just has a lot of peaks. Those also coincide with minima in the radius and point below in the magnetic regime and above in the electric one. Following the analysis made before, it is expected that greater absolute values of k to mean that the loops are more unstable. But that is not what happens in the magnetic regime. So, the relation between chirality and the total charge goes beyond this first interpretation.

In subsection 2.2, we saw how we could express the network energy through the energy-momentum tensor. We can do the same for the particular case of a circular loop.

$$E = \mu_0 a \int \tilde{U} \epsilon d\sigma \propto \left(\frac{\tau}{\tau_0}\right)^{\lambda} \frac{r}{\sqrt{1-\dot{r}^2}} \tilde{U}\left(y, \mathsf{k}\right) \tag{3.12}$$

The value of this expression for the several previous simulations is represented in Figure 3.6.

In Minkowski space-time, energy seems to be almost perfectly conserved. This can be shown analytically. If we derive the energy expression and use Equation 2.18 we get

$$\frac{\dot{E}}{E} = \lambda \tau^{\lambda-1} \left[c_T^2 - \left(1 + c_T^2\right) \dot{r}^2\right], \tag{3.13}$$

which clearly vanishes in Minkowski space-time. On the other hand, when the expansion of the Universe is taken into account, the energy starts oscillating. This may signal numerical limitations in the integration of the loop's evolution. However, as time passes, the amplitude of

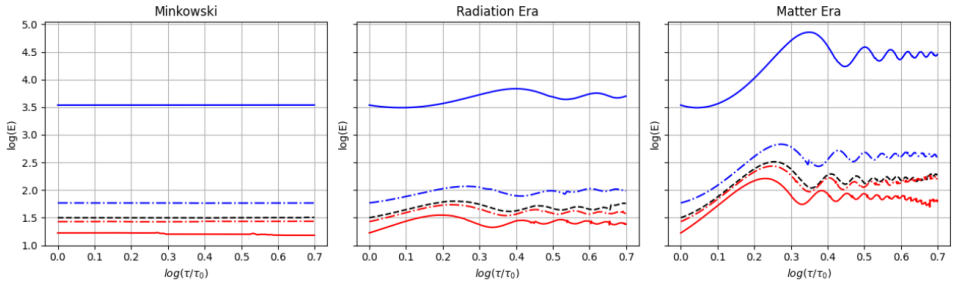


Figure 3.6: Energy values as a function of time in Minkowski space (left), in the radiation era (center) and in the matter era (right). Magnetic and electric regimes are represented by red and blue colors, respectively. The dashed and solid lines correspond to the Kaluza-Klein and Witten models. The linear model is represented by the dot-dashed black lines.

those oscillations seems to decrease, as if the energy is converging to some specific value. It's way more difficult to analyze these cases analytically, if not impossible.

One important aspect of Figure 3.6 is that the blue lines lie always above the red ones. And between the blue ones, the solid line is above the dashed and the opposite applies in the red. This agrees with our previous analysis if we relate greater energy values with a more stable environment. This makes sense. We can think that, when a loop disappears all its energy is lost (more specifically, the energy in the string, which is obvious). Well, if we start with a configuration with a greater energy, in principle, it will be more difficult for it to lose all of it (this argument should be carefully assimilated, because greater energy could lead to greater velocities, which, in more realistic cases, means an higher rate of energy losses).

4 Cosmic Strings Evolution in the Presence of an External Magnetic Field

In this chapter, I will study how cosmic strings evolve in the presence of an external magnetic field. I'll start by laying down the theoretical model and explain some considerations that were taken into account. I'll then look for scaling solutions and characterize the parameter space.

The initial goal of the work done in this chapter was to propose a reliable mechanism through which cosmic strings networks could gain energy, instead of losing it. Clearly any such process can not be dominant, otherwise it would be in direct opposition to the standard ΛCDM model characterizing the whole Universe.

4.1 The Model

In order to analyze the dynamical behavior of cosmic strings in a magnetic field background, we must allow an interaction between the field and the charges and currents within the string. All we have to do is to consider a coupling term between both quantities, which we have already seen in the effective action for superconducting strings, that we shall rewrite here, for demonstration purposes

$$S = -\mu_0 \int \left\{ \sqrt{-\gamma} - \frac{1}{2}\sqrt{-\gamma}\gamma^{ab}\varphi_{,a}\varphi_{,b} + eA_\mu x^\mu_{,a}\varepsilon^{ab}\varphi_{,b} \right\} d^2\sigma. \tag{4.1}$$

We can now relate this action to the CVOS formalism already studied in subsection 2.2. In fact the first two terms correspond to the linear model, where $f(\mathsf{k}) = 1 - \frac{\mathsf{k}}{2}$.

If we add the familiar kinetic term for the electromagnetic field to the previous action and vary it with respect to the potential gauge vectors, A_μ, we get the field equation

$$\nabla_\nu F^{\mu\nu} = -4\pi \mathsf{j}^\mu, \tag{4.2}$$

where the 4-current is given by $\mathsf{j}^\mu(y) = \int \sqrt{-\gamma} x^\mu_{,a} \mathcal{J}^a \delta^{(4)}(y - x(\sigma))\, d^2\sigma$ (as in [10] - which uses Gauss units; however we are dealing with an expanding Universe instead of Minkowski spacetime). In turn, $\mathcal{J}^a$ is the string worldsheet current and is defined as $\mathcal{J}^a = e\frac{\varepsilon^{ab}}{\sqrt{-\gamma}}\varphi_{,b}$. It is straightforward to determine the values of the charge and current in the string within this formalism. The charge corresponds to $\mathcal{J}^0 = \frac{e\varphi'}{a^2\sqrt{(1-\dot{\mathsf{x}}^2)\mathsf{x}'^2}}$, while the current is $\mathcal{J}^1 = -\frac{e\dot{\varphi}}{a^2\sqrt{(1-\dot{\mathsf{x}}^2)\mathsf{x}'^2}}$. The way it is defined, the worldsheet current is covariantly conserved

$$\nabla_a \mathcal{J}^a = \frac{1}{\sqrt{-\gamma}} \partial_a \left(\sqrt{-\gamma} \mathcal{J}^a \right) = \frac{e}{\sqrt{-\gamma}} \varepsilon^{ab} \partial_a \partial_b \varphi = 0. \tag{4.3}$$

At this point, the reader already realized that the charges and currents on the strings differ from the previously defined ones. This is not of vital importance for two main reasons:

- The first reason is related to the very elementary notion of charges and currents. Here the purpose is not to delve in a philosophical search for the understanding of such entities, but to think in a practical way. They appear, as they did in Equation 4.2, as source terms for the electromagnetic fields. And so, in the absence of such fields, their definition is a little dubious. For example, in the CVOS formalism, such questions were not raised, because we never had the need to invoke electromagnetic fields. Their interaction was hidden in the function f, and charge and current were added to apply some intuition. However, now we are in the presence of electromagnetic fields, and we want to study how strings evolve in the presence of a magnetic field. But again, the problem seems to fall depending on our assumptions. Here, we will be considering an external magnetic field which does not suffer backreaction from the charges and currents in the string. On the other hand, the field will affect the charges and currents, which leads us to the second argument;
- In this case, where both charges and currents are created through a scalar field, the problem is merely terminological. This is because, the charges and currents in the source term of equation Equation 4.2, and the equations of motion following the action 4.1 are written in terms of φ, and not of some inherent charge or current. Therefore, the terminology is hiding the true role of the scalar field.

And so, we have the conditions to continue with the definitions made in section 2.

As mentioned before, I will be considering an external magnetic field, **B**, which will not vary due to the scalar field. It does not need to be completely uniform or constant. However, any length or time scales for variations should be large enough in order for the charges and currents created on the strings, due to the magnetic field gradient or time derivative, to not be substantial.

The origin of the magnetic field is not of real importance. However we can consider two cases:

- Primordial magnetic fields can be generated in alternative models which describe the evolution of the Universe. As highlighted in [29], the origin mechanism falls into three broad classes: inflationary magnetic field generation; the generation of magnetic fields during phase transitions and magnetic fields from second order cosmological perturbation theory. These primordial fields would extend throughout all the Universe. However,

their intensity, if they exist, should be very low and very well constrained. [30] calculated an upper limit of 19 nG. Therefore, their contribution to the cosmic strings would not be dominant nor very substantial.

- Astrophysical magnetic fields. These reside in galaxies or in galaxy clusters, and, unlike the previous cases, they have been measured. They have their origin in the amplification of seed fields via dynamo processes. These seed fields can be generated by mechanisms such as the Biermann battery [31]. They could have a bigger contribution for the cosmic strings dynamics. However, they are not everywhere. One way to tackle this problem is to add a coefficient, less than one, to the additional magnetic field terms arising from our formulation. This coefficient could be given by the average fraction of volume occupied by galaxies inside a volume correspondent to the correlation length.

Anyway, the way electromagnetic fields are defined in a curved spacetime is not straightforward. We will be following [29, 32], which state $F_{\mu\nu} = u_\mu \mathcal{E}_\nu - u_\nu \mathcal{E}_\mu + \varepsilon_{\mu\nu\rho}\mathcal{B}^\rho$, where u^μ is the observer 4-velocity and $\varepsilon_{\mu\nu\rho} = u^\alpha \varepsilon_{\alpha\mu\nu\rho}$ is the totally antisymmetric tensor on the 3-space normal to u^μ, while $\varepsilon_{\alpha\mu\nu\rho}$ is the totally antisymmetric tensor in 4 dimensions with $\varepsilon_{0123} = \sqrt{-g}$. $\mathcal{E}$ and $\mathcal{B}$ are related to the electric and magnetic fields, respectively. In our case, considering the frame comoving with the Hubble flow, we get $u^\mu = \left(a^{-1}, 0, 0, 0\right)$. Assuming no electric field as well, and noting that the 3-vector magnetic field, **B**, is defined as $\mathcal{B}_\mu = a\,(0, \mathbf{B})$, we get for the antisymmetric tensor $F_{ij} = a^4 \tilde{\varepsilon}_{0ijk} g^{kl} B_l = -a^2 \tilde{\varepsilon}_{0ijk} \delta^{kl} B_l$, where $\tilde{\varepsilon}_{\alpha\mu\nu\rho} = \frac{\varepsilon_{\alpha\mu\nu\rho}}{\sqrt{-g}}$.

Varying the action 4.1 with respect to the scalar field, we get the following field equation

$$\frac{\partial}{\partial\tau}\left[a\frac{df}{d\mathsf{k}} q\sqrt{\mathsf{x}'^2}\right] - \frac{\partial}{\partial\sigma}\left[a\frac{df}{d\mathsf{k}} j\sqrt{1-\dot{\mathsf{x}}^2}\right] = \frac{1}{2} e a^2 \left(\dot{\mathbf{x}} \times \mathbf{B}\right) \cdot \mathbf{x}', \tag{4.4}$$

which clearly reduces to equation 2.20 for a vanishing magnetic field.

On the other hand, I proceeded, as usual, to determine the equations of motion. Then I acted with the velocity dot product on the spatial part of the equations, reading

$$\epsilon\tilde{U}\dot{\mathbf{x}}\cdot\ddot{\mathbf{x}} + \frac{\dot{a}}{a}\epsilon\dot{\mathsf{x}}^2\left(1-\dot{\mathsf{x}}^2\right)\left(\tilde{U}+\tilde{T}\right) - 2\Phi\dot{\mathbf{x}}'\cdot\dot{\mathbf{x}} - \epsilon\tilde{T}\left(1-\dot{\mathbf{x}}^2\right)\frac{\dot{\mathbf{x}}\cdot\mathbf{x}''}{\mathsf{x}'^2} = e\sqrt{1-\dot{\mathsf{x}}^2}\, q\left(\dot{\mathbf{x}}\times\mathbf{B}\right)\cdot\mathbf{x}', \tag{4.5}$$

which, again, reduces to equation 2.22 when **B** vanishes. It's important to note that the time equation is not affected by the presence of the magnetic field, and thus remains the same.

In both these equations (4.4, 4.5), the additional magnetic term is proportional to $(\dot{\mathbf{x}} \times \mathbf{B}) \cdot \mathbf{x}'$. This expression is reminiscent of the Lorentz force in the direction of the vortex. As the scalar

field is only defined on the cosmic strings, the net force provided by the magnetic field could only be on this direction.

4.2 Macroscopic Evolution

Once we get the microscopic description of the system we can average across the string network. The assumptions made are the same as in chapter section 2. There was no need to add more macroscopic quantities, and all of them are defined as before. The new network evolution equations read

$$\dot{L} = \frac{\dot{a}}{a}\frac{L}{W^2}\left\{\left[W^2 + \left(Q^2+J^2\right)F'\right]v^2 - \left(Q^2+J^2\right)F'\right\} + g\frac{\tilde{c}}{2}\frac{v}{W} \tag{4.6a}$$

$$\dot{v} = \frac{1-v^2}{W^2}\left\{\frac{k_v}{\xi}\left[W^2 - 2\left(Q^2+J^2\right)F'\right] - 2v\frac{\dot{a}}{a}\left[W^2 + \left(Q^2+J^2\right)F'\right] + eaBQ\theta\right\} \tag{4.6b}$$

$$\frac{dJ^2}{d\tau} = 2J^2\left[\frac{vk_v}{\xi} - \frac{\dot{a}}{a}\right] + \rho\tilde{c}\frac{v}{L}\frac{(g-1)W}{F' - 2Q^2F''} \tag{4.6c}$$

$$\frac{dQ^2}{d\tau} = 2Q^2\frac{F' + 2J^2F''}{F' + 2Q^2F''}\left[\frac{vk_v}{\xi} - \frac{\dot{a}}{a}\right](1-\rho)\,\tilde{c}\frac{v}{L}\frac{(g-1)W}{F' + 2Q^2F''} + \frac{eaBvQ\theta}{F' + 2Q^2F''}. \tag{4.6d}$$

As expected, turning off the magnetic field yields the same equations of CVOS. Only the velocity and the charge evolution were affected by the presence of the external magnetic field. It's straightforward for the current equation to not have an additional term, due to the way it is defined. On the other hand, at first glance, the characteristic lengthscale, which is a measure of the total energy of the network, should be affected. This feature comes from the fact that there is no additional term in the microscopic time equation of motion. However, we can relate this with the fact that any magnetic field has no work contribution. Nevertheless, L feels the presence of the magnetic field indirectly, through its dependence on the charge and velocity.

In these macroscopic equations, there appeared two new quantities related to the magnetic field. The first, B, can be seen as the effective mean intensity of the magnetic field, $\langle \mathbf{B} \rangle \equiv B\langle \hat{u} \rangle$, where $\hat{u}$ is a unit vector pointing in the direction of **B**. It should not be confused with the observer velocity, u^μ, in the definition of the Maxwell antisymmetric tensor nor with the vectors, $\tilde{u}^\mu$, defined to parameterize the energy-momentum tensor. The other parameter is θ and is given by

$$\theta = \left\langle \frac{(\dot{\mathbf{x}} \times \hat{u}) \cdot \mathbf{x}'}{\sqrt{\dot{\mathbf{x}}^2 \mathbf{x}'^2}} \right\rangle. \tag{4.7}$$

This value characterizes the interplay between the charge movement, the cosmic strings velocity and the magnetic field directions, and ranges from -1 to 1. It can be regarded as a

phenomenological parameter whose value can be extracted through numerical simulations.

4.3 Scaling Regime

The VOS macroscopic equations allow for solutions where the correlation lengthscale accompanies the rate expansion of the Universe, and the velocity tends to remain constant [16]. There are arguments for the existence of such solutions. In the CVOS formalism, these solutions were studied in [33, 34]. Here, I shall do the same, extracting some insight on the CVOS scaling solution. I should emphasize that here we will be dealing with the linear function f, instead of the more general case explored in subsection 2.2.

I'll not particularly search for scaling solutions where the correlation length scales as $\frac{\xi}{\tau} = const.$ Instead, I'll follow [33], in order to find a broader set of solutions, where the relevant parameters scale as a power of the conformal time. This is a good ansatz, specially if the scale factor is also proportional to a power of τ, which happens in the radiation and in the matter era.

We will be considering solutions of the type

$$L = L_0 \tau^{\alpha} \tag{4.8a}$$

$$v = v_0 \tau^{\beta} \tag{4.8b}$$

$$Q = Q_0 \tau^{\gamma} \tag{4.8c}$$

$$J = J_0 \tau^{\delta} \tag{4.8d}$$

$$\xi = \xi_0 \tau^{\epsilon} \tag{4.8e}$$

The exponents were chosen to mimic the first letters of the greek alphabet, and should not be confused with previous microscopic string parameters denoted by the same symbols. Besides these ones, we have for the scale factor, $a = a_0 \tau^{\lambda}$, where $\lambda = 1, 2$ for the radiation and matter era, respectively. We can also allow for the magnetic field intensity to evolve as a power-law, $B = B_0 \tau^{p-2\lambda}$. The extra factor in the exponent is to make the conformal magnetic field, as introduced in [35], $B_c = a^2 B$ to scale as $B_c \propto \tau^p$.

The correlation length cannot scale faster than the Hubble radius. This implies $\epsilon \leq 1$. Similarly, the characteristic lengthscale cannot scale faster than the correlation lengthscale. If it did, eventually, L would be greater than ξ, meaning that the bare string energy would be greater than the total one, which does not make sense.

Substituting this ansatz into eqs. 4.6, we get the rather unpleasant set

$$\alpha = \lambda\left[v_0^2\tau^{2\beta} + \frac{1}{2}\frac{L_0^2}{\xi_0^2}\mathcal{D}_0^2 C_v \tau^{2(\alpha-\epsilon+\eta)}\right] + \frac{g\tilde{c}}{2}\frac{v_0}{\xi_0}\tau^{1+\beta-\epsilon} \tag{4.9a}$$

$$\frac{\beta v_0}{C_v} = \frac{k_v}{\xi_0}\left[1 - \frac{L_0^2}{\xi_0^2}\mathcal{D}_0\tau^{2(\alpha-\epsilon+\eta)}\right]\tau^{1-\beta-\epsilon} - 2v_0\lambda\left[1 - \frac{1}{2}\frac{L_0^2}{\xi_0^2}\mathcal{D}_0\tau^{2(\alpha-\epsilon+\eta)}\right] + \frac{L_0^2}{\xi_0^2}Q_0\Delta\tau^{2\alpha-2\epsilon+1+\gamma-\lambda-\beta+p} \tag{4.9b}$$

$$\delta = \frac{v_0 k_v}{\xi_0}\tau^{1+\beta-\epsilon} - \lambda - \rho\,(g-1)\,\tilde{c}\frac{v_0\xi_0}{J_0^2 L_0^2}\tau^{1+\beta+\epsilon-2\alpha-2\delta} \tag{4.9c}$$

$$\gamma = \frac{v_0 k_v}{\xi_0}\tau^{1+\beta-\epsilon} - \lambda - (1-\rho)\,(g-1)\,\tilde{c}\frac{v_0\xi_0}{Q_0^2 L_0^2}\tau^{1+\beta+\epsilon-2\alpha-2\gamma} - \frac{v_0}{Q_0}\Delta\tau^{1+\beta-\gamma-\lambda+p}. \tag{4.9d}$$

It is important to note that what we are trying to do is to describe analytically the behavior of these macroscopic quantities, when the string network reaches the scaling regime. In other words, we are trying to determine the final asymptotic profile of the previous parameters. Therefore, it is expected that this regime happens for 'large' values of τ. In this analysis, there will be times when we will be considering the limit $\tau \to \infty$.

Examples tackling this situation are the definitions of $\mathcal{D}_0^2$ and of C_v. The first one comes from the expression $Q^2 + J^2 = Q_0^2\tau^{2\gamma} + J_0^2\tau^{2\delta}$. If the charge grows faster than the current, then, in the limiting case, it will dominate the value, and vice-versa. If the exponents are equal, then both remain present. And therefore, we have:

$$\mathcal{D}_0^2 = \begin{cases} Q_0^2, & \text{if } \gamma > \delta \\ J_0^2, & \text{if } \gamma < \delta \\ Q_0^2 + J_0^2, & \text{if } \gamma = \delta \end{cases} \tag{4.10}$$

The exponent η is the largest one among γ and δ. Therefore, we would have $Q^2 + J^2 \to \mathcal{D}_0^2\tau^{2\eta}$.

The same thing happens with $C_v = 1 - v_0^2\tau^{2\beta}$. If $\beta > 0$, then, eventually, no matter the value of v_0, the velocity would be greater than 1. This is not possible, for causality reasons. And so, we must have $\beta \leq 0$. If $\beta = 0$, then $C_v = 1 - v_0^2$ is constant. If not, then $C_v \to 1$, and can be regarded as a constant as well.

The parameter Δ in the scaling equations is related with the magnetic field and is surprisingly useful. This is because the unknown parameters, e, a_0, $B_{c,0}$ and θ, appear always together and in the same manner. So we can hide the uncertainties of four parameters in a single phenomenological one, which is given by

$$\Delta = \frac{eB_{c,0}\theta}{a_0}. \tag{4.11}$$

Obviously, the case $\Delta = 0$ reduces to the CVOS model, and, therefore, is of secondary interest.

In order to find the scaling solutions, we have to play with the exponents of τ. If they all vanish, then we get our constants. However, this may not be possible, due to the various restrictions put into the parameters α, β, γ, δ and ϵ. From now on, we shall call these quantities our variables (although they must be constants). Nonetheless, we can give less stringent restrictions. It is not required for the exponents to vanish. We can also have them being less then 0. And we have to sail between this exponent interplay, in order to solve for our variables.

Not all exponents can be negative. The restriction above of Δ being different from 0, also implies that we cannot have the magnetic field exponents both less than 0. On the other side, the exponent in the velocity equation $1 - \beta - \epsilon \geq 0$, no matter what. What we cannot have are exponents greater than 0. However, when $\beta < 0$, we get $1 - \beta - \epsilon > 0$. Fortunately, this can be remedied, by forcing $\alpha - \epsilon + \eta = 0$ and $\frac{L^2}{\xi_0^2}\mathcal{D}_0^2 = 1$, and the whole term vanishes.

Before presenting the solutions that were found, there is one more restriction our variables should satisfy. It concerns the relationship between L and ξ. In this model, we still have $\frac{\xi}{L} = W = \sqrt{\left\langle \tilde{U} \right\rangle}$, where $\tilde{U}$ is calculated considering the linear function. $\tilde{U}$ continues to be the worldsheet energy density in the charge carriers. And so, we have

$$\frac{L_0^2}{\xi_0^2}\tau^{2(\alpha-\epsilon)} = \frac{2}{2 + \mathcal{D}_0^2\tau^{2\eta}}. \tag{4.12}$$

This condition provides with only three options, depending on the value of η.

- If $\eta = 0$, then we must have $\alpha = \epsilon$, which implies $\frac{L_0^2}{\xi_0^2} = \frac{2}{2+\mathcal{D}_0^2}$;
- If $\eta < 0$, then we must have $\alpha = \epsilon$ and $\frac{L_0^2}{\xi_0^2} = 1$;
- If $\eta > 0$, then we must have $\alpha - \epsilon + \eta = 0$ and $\frac{L_0^2}{\xi_0^2}\mathcal{D}_0^2 = 2$.

The last situation clashes with the condition for $\beta < 0$, already seen. Therefore, we can't have $\eta > 0$ and $\beta < 0$ at the same time. This restriction invalidates a substantial number of possible, more exotic solutions. If instead $\eta \leq 0$, then $\alpha = \epsilon$. But $\beta < 0$ implies $\alpha - \epsilon - \eta = 0$. So, for decaying velocity the only possibility is $\eta = 0$, which means no growing charge or current.

We should note that, this happens because we are considering the function f to be linear, as in the effective action for superconducting strings 4.1. If, instead, we would allow for higher order terms, eq. 4.12 would be a restriction on the behavior of F and F'.

4.4 Analytical Solutions

I found several solutions for the set of eqs 4.9 relating our variables. They are accompanied by restrictions on the 'initial' values of the different parameters (I'm referring to the parameters with the 0 index). The momentum parameter, k_v, is considered a constant. We will take the value of k_0 in the numerical simulations study [36], and $\tilde{c} = 0.23$, as already mentioned.

Due to some conditions already studied, the solutions can be packed in three different boxes:

- Constant velocity ($\beta = 0$) and $\eta \geq 0$. There are three solutions with these features and each one can be unfolded, in principle, into two different situations, whether $\eta = 0$ or $\eta > 0$;
- Constant velocity ($\beta = 0$) and $\eta < 0$. There is only one solution of this type, but again, it can be divided in two, wheter $\eta = \gamma$ or $\eta = \delta$. It is singular, as it is the only one which require $g = 1$;
- Decreasing velocity ($\beta < 0$) and $\eta = 0$. These conditions encompass the majority of solutions. In total, there exist six of this type.

4.4.1 $\beta = 0$ and $\eta \geq 0$

As previously mentioned, in this situation, there are 3 solutions. The first reads

$$\alpha = \lambda - p \tag{4.13a}$$

$$\beta = 0 \tag{4.13b}$$

$$\gamma = 1 - \lambda + p \tag{4.13c}$$

$$\delta = 1 - \lambda + p + \frac{v_0}{Q_0}\Delta + (g-1)\,\tilde{c}\frac{v_0\xi_0}{Q_0^2 L_0^2} \tag{4.13d}$$

$$\epsilon = 1. \tag{4.13e}$$

On lack of greater originality, this shall be called solution $A1$. It requires $\rho = 0$ and $\frac{v_0}{Q_0}\Delta + (g-1)\,\frac{v_0\xi_0}{Q_0^2 L_0^2} < 0$, so that $\eta = \gamma$ and $\mathcal{D}_0^2 = Q_0^2$. Unfolding in the two possible cases:

- If $\eta = 0$, then $p = \lambda - 1$, allowing to simplify our variables:

$$\alpha = \epsilon = 1 \tag{4.14a}$$

$$\gamma = 0 \tag{4.14b}$$

$$\delta = \frac{v_0}{Q_0}\Delta + (g-1)\,\frac{v_0\xi_0}{Q_0^2 L_0^2} < 0, \tag{4.14c}$$

with the constrains

$$\frac{g\tilde{c}}{2}\frac{v_0}{\xi_0} + \lambda\left[v_0^2 + \frac{Q_0^2}{2+Q_0^2}\left(1-v_0^2\right)\right] = 1 \tag{4.15a}$$

$$v_0\frac{k_v}{\xi_0} - (g-1)\,\tilde{c}\frac{Q_0^2}{2+Q_0^2}\frac{v_0}{\xi_0} - v_0\frac{\Delta}{Q_0} = \lambda \tag{4.15b}$$

$$\frac{k_v}{\xi_0}\left(2-Q_0^2\right) + 2Q_0\Delta = 4v_0\lambda \tag{4.15c}$$

This is a set of three equations. Knowing $\tilde{c}$, k_v and λ, and giving values for g and Δ, it is possible to solve the system for the three parameters v_0, Q_0 and ξ_0. The parameter space studied covered the regions between $0 < g < 2$ and $-2 < \Delta < 2$. In the radiation era, there were no regions where the three parameters would satisfy all the restrictions.

However, in the matter era, for $\lambda = 2$, such regions were found. And by comparing the values of v_0 and ξ_0, it was found a perfect linear correlation between both (I calculated the Pearson correlation, almost yielding the exact value of 1.0). By averaging, I got $\frac{v_0}{\xi_0} \approx 1.3$.

If we look with attention to the second restriction, we can see that we can rewrite $\delta = v_0\frac{k_v}{\xi_0} - \lambda$. And therefore, the evolution of the current is very well restrained, with $\delta = -0.3$.

Another interesting feature are the possible energy fraction values. From the previous analysis, $\frac{E_0}{E} = \frac{2}{2+Q_0^2}$. The plot featuring this against the velocity squared values can be seen in Figure 4.1. As expected [18], featureless strings, with a lesser contribution from charge and currents, have a greater velocity.

- If $\eta > 0$, the conditions, in addition to the values of the constants taken into considerations lead to a negative value of g. This would mean that the network would have an overall energy gain when loops are formed, which is unphysical, and therefore, cannot happen.

Following to the next solution, which shall be called $A2$, we have

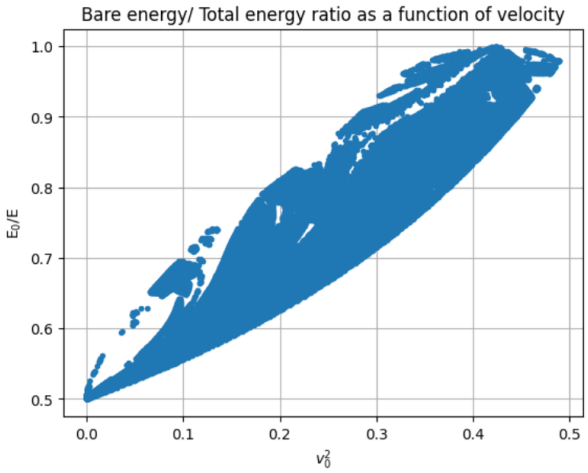


Figure 4.1: Ratio between the bare string energy E_0, and the total energy, E, as a function of the final velocity squared, v_0^2

$$\alpha = \lambda - p - \frac{v_0}{Q_0}\Delta + (g-1)\,\tilde{c}\frac{v_0\xi_0}{J_0^2 L^2} \tag{4.16a}$$

$$\beta = 0 \tag{4.16b}$$

$$\gamma = 1 - \lambda + p \tag{4.16c}$$

$$\delta = 1 - \lambda + p + \frac{v_0}{Q_0}\Delta - (g-1)\,\tilde{c}\frac{v_0\xi_0}{J_0^2 L^2} \tag{4.16d}$$

$$\epsilon = 1. \tag{4.16e}$$

It requires $\rho = 1$ and $\frac{v_0}{Q_0}\Delta - (g-1)\,\tilde{c}\frac{v_0\xi_0}{J_0^2 L^2} > 0$. Studying the two cases:

- If $\eta = 0$, then $p = \lambda - 1 - \frac{v_0}{Q_0}\Delta + (g-1)\,\tilde{c}\frac{v_0\xi_0}{J_0^2 L^2}$. This implies $\alpha = \epsilon = 1$ and $\gamma < 0$. The set of restrictions are the following

$$\frac{g\tilde{c}}{2}\frac{v_0}{\xi_0} = 1 - \lambda + \frac{2}{2+J_0^2}\left(1 - v_0^2\right)\lambda \tag{4.17a}$$

$$\frac{k_v}{\xi_0}\left(2 - J_0^2\right) = 4v_0\lambda \tag{4.17b}$$

$$v_0\frac{k_v}{\xi_0} = \lambda + (g-1)\,\frac{\tilde{c}}{2}\frac{v_0}{\xi_0}\frac{2+J_0^2}{J_0^2} \tag{4.17c}$$

$$p < \lambda - 1 \tag{4.17d}$$

$$\frac{L_0^2}{\xi_0^2}J_0^2 = \frac{2J_0^2}{2+J_0^2}. \tag{4.17e}$$

We can solve for v_0, J_0 and ξ_0, by varying g and $\frac{\Delta}{Q_0}$ (we could also vary p; at the end it would be the same thing as, in this case, it is closely related to $\frac{\Delta}{Q_0}$).

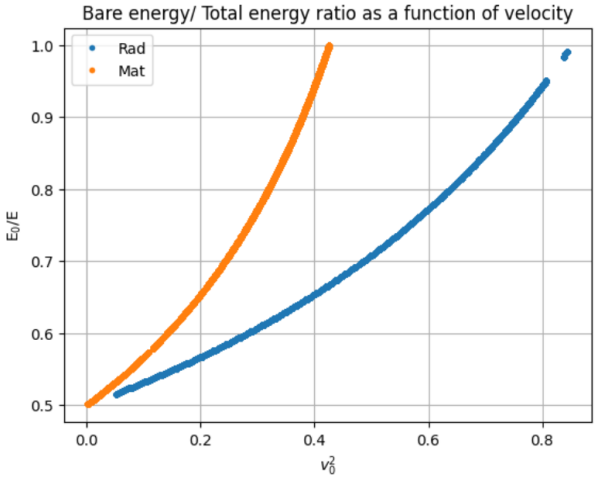


Figure 4.2: Ratio between the bare string energy E_0, and the total energy, E, as a function of the final velocity squared, v_0^2, in the radiation (blue dots) and matter (orange dots) eras, considering solution $A2$.

For the radiation era, we found a huge correlation between v_0 and ξ_0. They are proportional and $\frac{v_0}{\xi_0} \approx 1.3$. The standard deviation is of the order 1×10^{-10}. In the same way, J_0^2 is also strongly correlated with the velocity squared, and we get the same behavior for the energy content as a function of the velocity, as it can be seen in Figure 4.2 (in this case the energy ratio seems to be well more restrained for a given velocity).

On the other hand, the charge evolves in a broader way. Its exponent vary between $-2.9 < \gamma < 0$.

For $\lambda = 2$, the solution yields the same results. In fact, we continue to have $-2.9 < \gamma < 0$, $\frac{v_0}{\xi_0} \approx 1.3$ and the energy profile remains the same, as it can be seen in Figure 4.2. The only difference seems to be the range of the velocity values, with $v_0^2 \lesssim 0.5$. This is probably a consequence of the higher Hubble damping term.

- Again, if $\eta > 0$, we arrive at an absurdity. However, instead of being the values of the constants ruling out the solution, this time, the conditions themselves imply $k_v = 0$, which is only expected in Minkowski space, which is not studied here.

The last solution which satisfy $\beta = 0$ and $\eta \geq 0$ allows for a greater freedom on the value of ρ and requires $\gamma = \delta$ (which implies $\mathcal{D}_0^2 = Q_0^2 + J_0^2$). The solution $A3$ reads

$$\alpha = \lambda - p \tag{4.18a}$$

$$\beta = 0 \tag{4.18b}$$

$$\gamma = 1 - \lambda + p \tag{4.18c}$$

$$\delta = 1 - \lambda + p \tag{4.18d}$$

$$\epsilon = 1. \tag{4.18e}$$

- If $\eta = 0$, then $p = \lambda - 1$, $\alpha = \epsilon = 1$ and $\gamma = \delta = 0$. These result in the following restrictions

$$\frac{2}{2 + Q_0^2 + J_0^2}\left(1 - v_0^2\right)\lambda - \frac{g\tilde{c}}{2}\frac{v_0}{\xi_0} = \lambda - 1 \tag{4.19a}$$

$$\frac{k_v}{\xi_0}\left(2 - Q_0^2 + J_0^2\right) - 4v_0\lambda + 2Q_0\Delta = 0 \tag{4.19b}$$

$$v_0\frac{k_v}{\xi_0} - \rho\,(g-1)\,\tilde{c}\frac{v_0}{\xi_0}\frac{2 + Q_0^2 + J_0^2}{2J_0^2} = \lambda \tag{4.19c}$$

$$v_0\frac{\Delta}{Q_0} = \left[\frac{\rho}{J_0^2} - \frac{1-\rho}{Q_0^2}\right](g-1)\,\tilde{c}\frac{v_0}{\xi_0}\frac{2 + Q_0^2 + J_0^2}{2}. \tag{4.19d}$$

I studied this solution for the two values $\rho = 0, 1$. In the first case, considering the radiation era, we got $\frac{v_0}{\xi_0} \approx 0.76$, again with an uncertainty of the order 10^{-10}. There is not a clear profile of the energy ratio anymore. However, it can be noted an incredible decreasing on the bare string energy, with $\frac{E_0}{E}$ being very close to 0. Against what should be expected, the strings are highly relativistic, with $v_0^2 > 0.95$. In the matter era, $\frac{v_0}{\xi_0} \approx 1.52$, which is twice the radiation era value. The bare string energy rose again, accompanied with more moderated velocity values, $v_0^2 < 0.8$.

For $\rho = 1$, all the previous features disappear. There is no correlation between any parameter, and no way to establish a relation between the energy fraction and the velocity. This happens for both the radiation and the matter era.

- If $\eta > 0$, then $p > \lambda - 1$ and the parameters must satisfy

$$\frac{g\tilde{c}}{2}\frac{v_0}{\xi_0} = -p \tag{4.20a}$$

$$\frac{k_v}{\xi_0} = 2\frac{Q_0\Delta}{Q_0^2+J_0^2} \tag{4.20b}$$

$$v_0\frac{k_v}{\xi_0} - \rho\,(g-1)\,\frac{\tilde{c}}{2}\frac{v_0}{\xi_0}\frac{Q_0^2+J_0^2}{J_0^2} = 1+p \tag{4.20c}$$

$$v_0\frac{\Delta}{Q_0} = \left[\frac{\rho}{J_0^2} - \frac{1-\rho}{Q_0^2}\right](g-1)\,\tilde{c}\frac{v_0}{\xi_0}\frac{Q_0^2+J_0^2}{2}. \tag{4.20d}$$

The first condition implies $p < 0$, which means that $\lambda < 1$. This does not correspond to neither the radiation or the matter era. However, it is needed if we want to have v_0 and ξ_0 both positive. This set of conditions depends on the values of several quantities, such as Δ, g, ρ and p. This leads to a enormous parameter space to study. However, in order to be able to draw some relation to the other cases already studied, we will consider $\rho = 0$ or $\rho = 1$. The case for $\rho = \frac{1}{2}$ is also analyzed. In all cases, p can be written in terms of g, decreasing the parameter space.

Analytical solutions can be drawn from these three cases. For $\rho = 0$, the previous conditions would imply $g < 0$, which is impossible.

For $\rho = 1$, we get $\frac{v_0}{\xi_0} = \frac{2}{k_v+\tilde{c}} \approx 1.3$. This may allow us to explain the value of $\frac{v_0}{\xi_0}$ in the first two cases. The ratio between the 'initial' current and charge is $\frac{J_0^2}{Q_0^2} = \frac{(g-1)\tilde{c}}{k_v}$, which implies that $g > 1$. The evolution of the magnetic field is also restricted, $p = -\frac{g\tilde{c}}{k_v+\tilde{c}}$. This has implications on the possible expansion rates of the Universe. More specifically, $\lambda < \frac{k_v}{k_c+\tilde{c}} \approx 0.86$. We can also determine the values of $\alpha = \lambda + \frac{g\tilde{c}}{k_v+\tilde{c}}$, getting $0.15 \lesssim \alpha \leq 1$, with the minimum happening for $g \to 1^+$ and $\lambda \to 0^+$.

For $\rho = \frac{1}{2}$, there are a lot of similarities. In fact, $\frac{v_0}{\xi_0} = \frac{2}{k_v+\tilde{c}} \approx 1.3$. The ratio between charge and current changes a bit, $\frac{Q_0^2}{J_0^2} = \frac{2k_v}{(g-1)\tilde{c}} + 1$, which implies $g > 1 - \frac{2k_v}{\tilde{c}}$. However this value is negative, and therefore, $g > 0$ is valid. The range upon which the expansion rate is submitted is $\lambda < 1$. In turn, α varies between 0 and 1.

In this case, the energy ratio profile is not very relevant, because as $\eta > 0$, $\frac{E_0}{E} \to 0$ (this also explains why, in opposition to the $\eta = 0$ cases, it was not possible to determine the value of $\mathcal{D}_0^2$).

Although it was not possible to draw some conclusions relating the solutions, it was important to highlight a kind of symmetry. $A1$ demands $\gamma > \delta$ and $\mathcal{D}_0^2 = Q_0^2$; $A2$ requires $\gamma < \delta$ and $\mathcal{D}_0^2 = J_0^2$ and in $A3$ we have $\gamma = \delta$ and $\mathcal{D}_0^2 = Q_0^2 + J_0^2$. Each solution tackles a different charge

and current relation. In addition, it is important to note that $\gamma > \delta \Rightarrow \rho = 0$, $\gamma < \delta \Rightarrow \rho = 1$ and $\gamma = \delta \Rightarrow 0 \leq \rho \leq 1$. There seems to be an interplay between the dominant quantity $\mathcal{D}_0^2$ and the bias parameter.

If the charge grows faster than the current, then regions with greater charge will lose more energy, due to loop formation. Obviously, these energy losses will always be present (because, in this case, the charge will always dominate over the current). The same happens when the current grows faster than the charge. We should note that, in both these cases, where $\rho = 0, 1$, i. e., where energy losses due to loops formation are solely dependent on the charge or the current, exclusively, we couldn't find a $\eta > 0$ regime. This is perhaps a consequence of the strong loop production (in other words, for the case of $\rho = 0$: in these strings, the charge is greater than the current; regions with greater charge are more prone to form loops, which lead to energy and charge losses - this process may explain why the charge does not grow over time).

However, if $\gamma = \delta$, the bias parameter has a greater distribution. The fact that both the charge and current evolve at the same rate, does not mean one cannot dominate the other. It will all depend on the values of J_0^2 and Q_0^2. If the previous analysis was correct, when $J_0^2 \ll Q_0^2$, we would expect smaller values of ρ, and vice-versa (for $\eta = 0$). When $J_0^2 \approx Q_0^2$ or $\eta > 0$, the interplay between these values and the bias parameter seems more complex.

Before passing to the next solutions, we should mention that, in the limiting case of a vanishing magnetic field, $\Delta \to 0$, solutions $A1$, $A2$ and $A3$ (in the case of $\eta = 0$) converge to equations (39), (37) and (30) of the paper [34], respectively. This is to be expected once in this article, the author proposed to study CVOS scaling solutions.

4.4.2 $\beta = 0$ and $\eta < 0$

This subsection treats the only solution for decaying charge and current. This means that the energy is given by the bare string energy, $\frac{E_0}{E} \to 1$. There is only one solution with these features, which shall be called solution B

$$\alpha = \epsilon = 1 \tag{4.21a}$$

$$\beta = 0 \tag{4.21b}$$

$$\gamma = 1 - \lambda + p \tag{4.21c}$$

$$\delta = 1 - \lambda + p + \frac{v_0}{Q_0}\Delta. \tag{4.21d}$$

The restrictions will vary whether $\gamma > \delta$ or $\gamma < \delta$. These situations correspond to having $\Delta < 0$ or $\Delta > 0$, respectively. The case of a vanishing magnetic field would imply $\gamma = \delta$.

It is important to highlight that this solution is only possible if $g = 1$. This makes sense, because g characterizes how regions with charges and currents lose energy due to loop formation. For a vanishing charge and current, we couldn't have otherwise. In the same way, with no Q and J, the bias parameter is ill-defined. And this also happens precisely when $g = 1$.

- If $\Delta < 0$, then we have

$$\lambda > \frac{2}{1+\frac{\tilde{c}}{k_v}} \approx 1.7 \tag{4.22a}$$

$$v_0^2 = \frac{1}{1+\frac{\tilde{c}}{k_v}} \frac{1}{\lambda} < \frac{1}{2} \tag{4.22b}$$

$$\frac{v_0}{\xi_0} = \frac{2}{k_v + \tilde{c}} \approx 1.3 \tag{4.22c}$$

$$p = 1 - \frac{2\tilde{c}}{k_v + \tilde{c}} - \frac{v_0}{Q_0}\Delta. \tag{4.22d}$$

  We retrieve the already seen $\frac{v_0}{\xi_0}$ value. On the other hand, the value of p is related to Δ, and therefore we can have the magnetic field evolving in a large range of ways. We should also note the restriction on the strings velocity. Ultra-relativistic regimes are not allowed. However, the most notable feature is the large expansion rates allowed. In opposition to the previous case, where $\eta > 0$ would require $\lambda \lesssim 0.86$ (in solution $A3$), now we must have $\lambda \gtrsim 1.7$, so including the matter era but not the radiation era. This is needed to dilute away the charge and current content.

- If $\Delta < 0$, the conditions remain the same, all but one. Instead, we have $\lambda > \frac{2}{1+\frac{\tilde{c}}{k_v}} - \frac{v_0}{Q_0}\Delta > \frac{2}{1+\frac{\tilde{c}}{k_v}} \approx 1.7$. So, in the end, we got the same behavior, although, if we want to be rigorous, now it is more difficult (we need even larger expansion rates) to dilute Q and J.

4.4.3 $\beta < 0$

This is the most populated subbranch of solutions: there is 6. As it was already mentioned before, a decaying velocity implies $\eta = 0$. At first sight, depending on the values of $\mathcal{D}_0^2$, the bare string energy to the total energy ratio must vary. However, for $\beta < 0$, we need $\frac{L_0^2}{\xi_0^2}\mathcal{D}_0^2 = 1$ (in order to make the growing power term in the velocity equation to vanish). On the other hand, $\eta = 0 \Rightarrow \frac{L_0^2}{\xi_0^2} = \frac{2}{2+\mathcal{D}_0^2}$. The two can only be reconciled if $\mathcal{D}_0^2 = 2$. This is a very specific value and corresponds exactly to an equal partition between the bare string and charge and current

energy contributions. In other words, $\frac{E_0}{E} = \frac{1}{2}$. All solutions are valid for $g \neq 1$, although for some, that is a necessary condition.

I'll start with the solution $C1$, which reads

$$\alpha = \epsilon = \frac{\lambda}{2} + \frac{g\tilde{c}}{2}\frac{v_0}{\xi_0} \tag{4.23a}$$

$$\beta = \gamma = -1 + \frac{\lambda}{2} + \frac{g\tilde{c}}{2}\frac{v_0}{\xi_0} \tag{4.23b}$$

$$\delta = 0. \tag{4.23c}$$

And the restrictions are the following

$$\rho = 1 \tag{4.24a}$$

$$\frac{g\tilde{c}}{2}\frac{v_0}{\xi_0} = 1 - \frac{3}{2}\lambda + \frac{Q_0\Delta}{2v_0} \tag{4.24b}$$

$$\frac{v_0}{\xi_0} = \frac{\lambda}{k_v - (g-1)\,\tilde{c}} \tag{4.24c}$$

$$v_0\frac{\Delta}{Q_0} = \left(k_c - \frac{g\tilde{c}}{2}\right)\frac{v_0}{\xi_0} + \frac{3}{2}\lambda \tag{4.24d}$$

$$\left[1 + \frac{g\tilde{c}}{k_v - (g-1)\,\tilde{c}}\right]\lambda < 2. \tag{4.24e}$$

If we want to have $\frac{v_0}{\xi_0} > 0$, we must have $g < 1 + \frac{k_v}{\tilde{c}}$. On the other hand, the last condition implies $g < \left(1 + \frac{k_v}{\tilde{c}}\right)(2 - \lambda)$, which accounting for a positive g, is only possible for $\lambda < 2$.

The parameter space and the possible values of α are represented in Figure 4.3. They seem to vary between 0 and 1, as it is expected. Regions where $\lambda > 1$ turned out to not belong to the parameter space.

Continuing, solution $C2$ reads

$$\alpha = \epsilon = \frac{\lambda}{2} + \frac{g\tilde{c}}{2}\frac{v_0}{\xi_0} \tag{4.25a}$$

$$\beta = -1 + \frac{\lambda}{2} + \frac{g\tilde{c}}{2}\frac{v_0}{\xi_0} \tag{4.25b}$$

$$\gamma = (g-1)\,\tilde{c}\frac{v_0}{\xi_0} \tag{4.25c}$$

$$\delta = 0 \tag{4.25d}$$

Before passing to the restrictions we can already see that $g < 1$, in order to have $\gamma < \delta$.

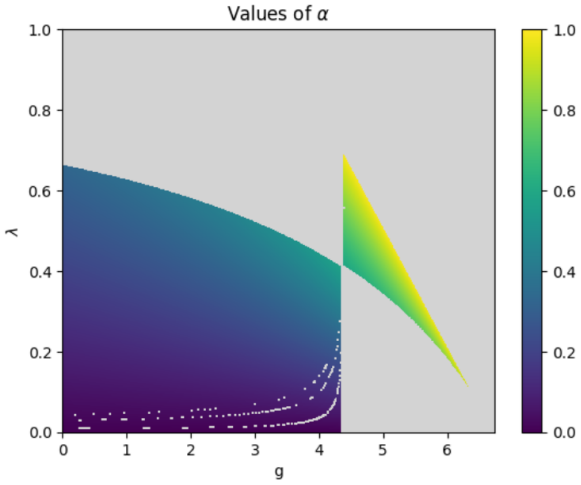


Figure 4.3: Possible values of α and ϵ considering the solution $C1$. Regions in gray do not belong to the parameter space.

The conditions are

$$\rho = 1 \tag{4.26a}$$

$$\frac{v_0}{\xi_0} = \frac{\lambda}{k_v} \tag{4.26b}$$

$$\frac{Q_0 \Delta}{v_0} = 3\lambda - 2 + g\tilde{c}\frac{v_0}{\xi_0} \tag{4.26c}$$

$$\left[1 + \frac{g\tilde{c}}{2k_v} - 2\left(g-1\right)\frac{\tilde{c}}{k_v}\right]\lambda < 2. \tag{4.26d}$$

By solving the last inequality for g and remembering that $g < 1$, we can restrain the expansion rate. More specifically, we get $\lambda < \frac{4}{2+\frac{\tilde{c}}{k_v}} \approx 1.84$. Therefore, this solution is not allowed in the matter era. Again, I'll study the parameter space by varying g and λ. The value of α is represented in Figure 4.4 and is obviously greater for bigger values of λ and g.

The next solution, $C3$, is characterized by

$$\alpha = \epsilon = 1 - \lambda \tag{4.27a}$$

$$\beta = -\lambda \tag{4.27b}$$

$$\gamma = -v_0\frac{\Delta}{Q_0} + \left(g-1\right)\tilde{c}\frac{v_0}{\xi_0} \tag{4.27c}$$

$$\delta = 0. \tag{4.27d}$$

This one is rather peculiar, because the restrictions don't allow us to determine all the relevant parameters:

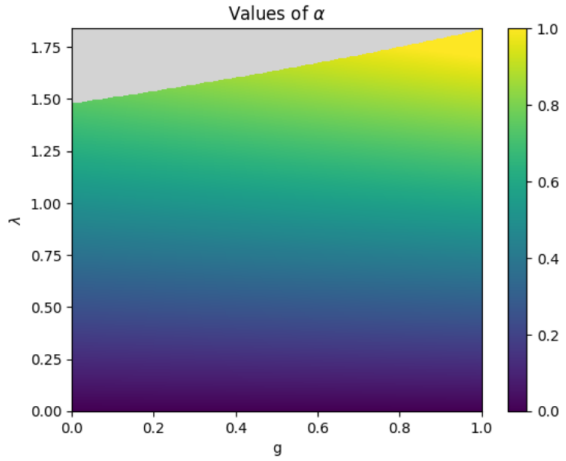


Figure 4.4: Possible values of α considering the solution $C2$. Regions in gray do not belong to the parameter space

$$\rho = 1 \tag{4.28a}$$

$$\frac{v_0}{\xi_0} = \frac{2}{3k_v + 3\tilde{c} - 2g\tilde{c}} \tag{4.28b}$$

$$\lambda = 2\frac{k_v + \tilde{c} - g\tilde{c}}{3k_v + 3\tilde{c} - 2g\tilde{c}} \tag{4.28c}$$

$$p = 2\lambda - 1 - v_0\frac{\Delta}{Q_0} + (g-1)\,\tilde{c}\frac{v_0}{\xi_0} \tag{4.28d}$$

$$v_0\frac{\Delta}{Q_0} > v_0\frac{k_v}{\xi_0} \tag{4.28e}$$

The parameter space reduces then to the g axis. In order to have $\lambda > 0$, we must have $g < 1 + \frac{k_v}{\tilde{c}}$. In turn, this implies $\frac{v_0}{\xi_0} > 0$, as it should be. It is not possible to determine the values of p and $v_0\frac{\Delta}{Q_0}$, although we know they are related. As a consequence, we also cannot calculate the possible values of γ, which must be negative. However, as it is usual in the solutions of this subsection, there is a roof on the value of the expansion rate of the Universe and can be deduced, $\lambda < \frac{2}{3}$. This restricts the possible values of α to lie between $\frac{1}{3}$ and 1.

These solutions, $C1$, $C2$ and $C3$, all required $\rho = 1$. And, with no coincidence, and similarly to the previous study of solutions $A1$, $A2$ and $A3$, all were dominated by the current. The charge had a vanishing asymptotic value.

There are three remaining solutions. One, $C4$, requires $\rho = 0$ and $\mathcal{D}_0^2 = Q_0^2$, as it is expected. For the other two, $\gamma = \delta$ and $\rho = \frac{J_0^2}{J_0^2+Q_0^2}$.

Solution $C4$ reads

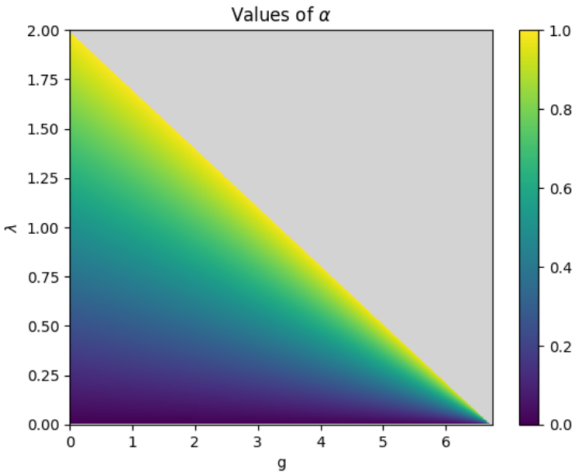


Figure 4.5: Possible values of α considering the solution $C4$. Regions in gray do not belong to the parameter space

$$\alpha = \epsilon = \frac{\lambda}{2} + \frac{g\tilde{c}}{2}\frac{v_0}{\xi_0} \tag{4.29a}$$

$$\beta = -1 + \frac{\lambda}{2} + \frac{g\tilde{c}}{2}\frac{v_0}{\xi_0} \tag{4.29b}$$

$$\gamma = 0 \tag{4.29c}$$

$$\delta = (g-1)\,\tilde{c}\frac{v_0}{\xi_0}. \tag{4.29d}$$

This solution seems to be a mirror image of $C2$. The differences lie in the change between γ and δ, and in some restrictions

$$\rho = 0 \tag{4.30a}$$

$$\frac{v_0}{\xi_0} = \frac{\lambda}{k_v - (g-1)\,\tilde{c}} \tag{4.30b}$$

$$\frac{Q_0\Delta}{v_0} = 3\lambda - 2 + g\tilde{c}\frac{v_0}{\xi_0} \tag{4.30c}$$

$$p = \frac{3}{2}\lambda - 2 + \frac{g\tilde{c}}{2}\frac{v_0}{\xi_0} \tag{4.30d}$$

$$\left[1 + \frac{g\tilde{c}}{k_v - (g-1)\,\tilde{c}}\right]\lambda < 2. \tag{4.30e}$$

We can study the parameter space by varying g and λ. The last condition implies $g < \left(1 + \frac{k_v}{\xi_0}\right)\left(1 - \frac{\lambda}{2}\right)$. In turn, g must be positive and therefore we have $\lambda < 2$. Again, α is represented in Figure 4.5 and, like in $C2$, it grows towards the top right corner. The range of values is similar when compared to Figure 4.4.

Now, we will move on to the final solutions, which have the particular feature of requesting $\rho = \frac{J_0^2}{J_0^2+Q_0^2}$. And so, solution $C5$ reads

$$\alpha = \epsilon = \frac{\lambda}{2} + \frac{g\tilde{c}}{2}\frac{v_0}{\xi_0} \tag{4.31a}$$

$$\beta = -1 + \frac{\lambda}{2} + \frac{g\tilde{c}}{2}\frac{v_0}{\xi_0} \tag{4.31b}$$

$$\gamma = \delta = 0 \tag{4.31c}$$

And again, this seems the extension of solutions $C2$ and $C4$, for the case where $\gamma = \delta$. The restrictions are the following

$$\rho = \frac{J_0^2}{J_0^2 + Q_0^2} \tag{4.32a}$$

$$\frac{v_0}{\xi_0} = \frac{\lambda}{k_v - (g-1)\,\tilde{c}} \tag{4.32b}$$

$$\frac{Q_0\Delta}{v_0} = 3\lambda - 2 + g\tilde{c}\frac{v_0}{\xi_0} \tag{4.32c}$$

$$p = \frac{3}{2}\lambda - 2 + \frac{g\tilde{c}}{2}\frac{v_0}{\xi_0} \tag{4.32d}$$

$$\left[1 + \frac{g\tilde{c}}{k_v - (g-1)\,\tilde{c}}\right]\lambda < 1, \tag{4.32e}$$

which, if it were for the last one, would be equal to the set of conditions imposed for solution $C4$. Again, as $g > 0$, we must have $\lambda < 1$. It's not possible to determine neither the charge or the current, and therefore the exact value of ρ is unknown. α is represented in Figure 4.6 and, we can see that it can not achieve the previous larger values. In fact, if we divide the last condition by 2, we can rewrite it as $\alpha < \frac{1}{2}$. The parameter space is also very similar to the one of solution $C4$.

The last solution, $C6$, is very different from what we are use to in this subsection. All but $C3$ have the same value for α, ϵ and β. The next one has also a very simple representation. Solution $C6$ reads

$$\alpha = \epsilon = \frac{\lambda}{2} \tag{4.33a}$$

$$\beta = -1 - \frac{\lambda}{2} \tag{4.33b}$$

$$\gamma = \delta = 0. \tag{4.33c}$$

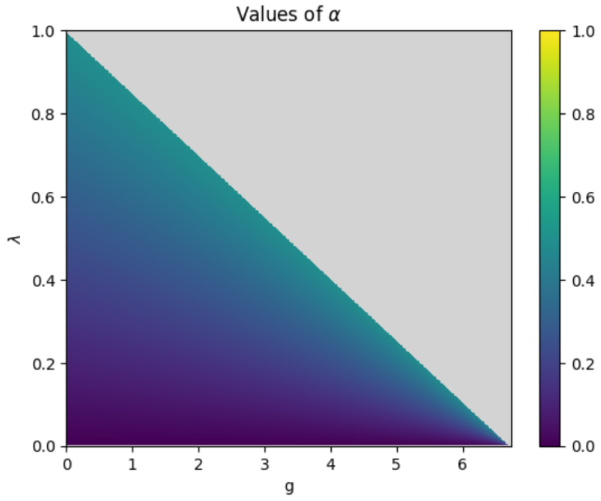


Figure 4.6: Possible values of α considering the solution $C5$. Regions in gray do not belong to the parameter space

The restrictions are in the same line as the ones in the previous solutions

$$\rho = \frac{J_0^2}{J_0^2 + Q_0^2} \tag{4.34a}$$

$$\frac{v_0}{\xi_0} = \frac{\lambda}{(g-1)\,\tilde{c}} \tag{4.34b}$$

$$\frac{Q_0 \Delta}{v_0} = \lambda - 2 \tag{4.34c}$$

$$p = \frac{\lambda}{2} - 2 \tag{4.34d}$$

$$\lambda < 2. \tag{4.34e}$$

So, in order to have $\frac{Q_0}{v_0} > 0$ and $\frac{v_0}{\xi_0} > 0$, we must have $\Delta < 0$ and $g < 1$. The parameter space is straightforward in this situation, corresponding to the square given by $0 < \lambda < 2$ and $0 < g < 1$. Although completely straightforward, the values of α are represented in Figure 4.7.

These solutions all have one thing in common. They need relatively low expansion rates, so the charge and current do not dilute away. For the majority the parameter space is very well parameterized by g and λ. Solutions $C2$, $C4$ and $C5$ seemed to be the same but for different regimes, $\delta > \gamma$, $\delta = \gamma$ and $\delta < \gamma$, respectively. $C1$ was not very different, yielding a more deformed parameter space. Solutions $C3$ and $C6$ were special in the sense that the variables α, ϵ and β were only dependent on λ.

It should also be noted that, until this subsection, all solutions required $\epsilon = 1$. These solutions could have $\epsilon < 1$, and so, the correlation length could scale at a slower rate when compared to the Hubble radius.

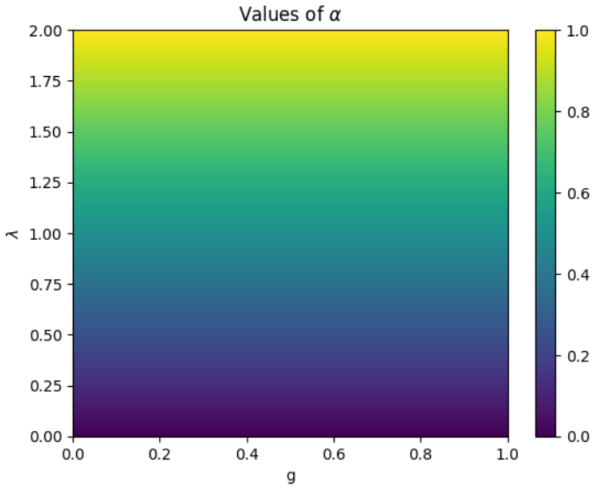


Figure 4.7: Possible values of α considering the solution $C6$.

5 Conclusion

In this thesis, we began by examining the microscopic equations of the CVOS model to describe the evolution of a circular current-carrying string. Our analysis showed that the inclusion of additional degrees of freedom — namely, internal charges and currents — can prevent the collapse of the loop and contribute to its long-term survival. We further investigated the role of cosmic expansion, finding that a higher expansion rate, through Hubble damping, enhances the dissipation of the loop's energy and thus promotes its decay.

One of the most unexpected and striking results, however, is the emergence of a more favorable stability landscape in the electric regime. Several independent indicators point towards enhanced robustness in this case, in contrast with the magnetic one. Still, as emphasized throughout the work, these findings must be interpreted with caution due to the absence of microscopic loss terms in the model, which could alter the dynamics significantly.

As a future line of research, we intend to incorporate these loss terms into the model, allowing for the characterization of energy dissipation through electromagnetic radiation. This extension is essential for a more realistic description of current-carrying loop dynamics. A framework for this kind of analysis was already explored in [37], which will serve as a foundation for our forthcoming developments.

In the final part, the main goal was to find a mechanism through which a current-carrying cosmic string network could recover energy. We explored the formalism of previous models, such as VOS and CVOS, and extended them to include the effect of an external, time-varying magnetic field. This new approach requires some fine-tuning, particularly with respect to the macroscopic quantity θ.

As it was already done in the literature, once we had the macroscopic equations describing the string network evolution, we searched for scaling solutions. We found a correlation between the value of the bias parameter ρ and the dominant quantity among the charge or current. An organized summary of all the solutions is presented in Table 5.1.

Although our purpose was to find a mechanism so the strings could gain energy, we only found one solution where the bare string energy would vanish asymptotically (and the energy present on the charge and current would dominate). This is, I think, a consequence of the strict restriction given by Equation 4.12. However, this comes from considering the linear function on the action 4.1. Initially those terms, accompanied with the coupling one, described the dynamics of the charge and currents on the string. However, this interplay was mimicked by the function f, in CVOS. Furthermore, we only used the coupling term to determine the influence of the

	$A1$	$A2$	$A3$	B	$C1$	$C2$	$C3$	$C4$	$C5$	$C6$
α	1	1	$[0,1]$	1	$[0,1]$	$[0,1]$	$\left[\frac{1}{3},1\right]$	$[0,1]$	$\left[0,\frac{1}{2}\right]$	$[0,1]$
ϵ	$=\alpha$	$=\alpha$	1	$=\alpha$	$=\alpha$	$=\alpha$	$=\alpha$	$=\alpha$	$=\alpha$	$=\alpha$
β	0	0	0	0	<0	<0	<0	<0	<0	<0
γ	0	$]-2.9,0[$	≥ 0	<0	<0	<0	<0	0	0	0
δ	≈ -0.3	0	$=\gamma$	<0	0	0	0	<0	$=\gamma$	$=\gamma$
λ	-	-	<1	$\gtrsim 1.7$	$\lesssim 0.8$	$\lesssim 1.84$	$<\frac{2}{3}$	<2	<1	<2

Table 5.1: Brief summary of the most important features of the solutions found in section 4. The possible values of λ in the solutions $A1$ and $A2$ were not studied. The λ interval in the $A3$ column corresponds to the case where $\eta > 0$.

magnetic field on the string, and not of the charges and currents on themselves. So a future model should take this into account, by changing the linear terms in Equation 4.1 by the function f. This would lend more insight as it would enable a broader class of solutions.

Another important direction for future work is the comparison between all analytical scaling solutions and full numerical simulations. Such an approach would enable a more precise calibration of the phenomenological parameters and provide a consistency check for the large-scale behavior of the string network.

References

[1] T. W. B. Kibble. Topology of cosmic domains and strings. *J. Phys. A*, 9:1387–1398, 1976.

[2] M. B. Hindmarsh and T. W. B. Kibble. Cosmic strings. *Rept. Prog. Phys.*, 58:477–562, 1995.

[3] Tomáš Brauner. Effective Field Theory for Spontaneously Broken Symmetry. *Lect. Notes Phys.*, 1023:pp., 2024.

[4] J. Goldstone. Field Theories with Superconductor Solutions. *Nuovo Cim.*, 19:154–164, 1961.

[5] Holger Bech Nielsen and P. Olesen. Vortex Line Models for Dual Strings. *Nucl. Phys. B*, 61:45–61, 1973.

[6] Edward Witten. Superconducting Strings. *Nucl. Phys. B*, 249:557–592, 1985.

[7] Graham Vincent, Nuno D. Antunes, and Mark Hindmarsh. Numerical simulations of string networks in the Abelian Higgs model. *Phys. Rev. Lett.*, 80:2277–2280, 1998.

[8] J. R. C. C. C. Correia and C. J. A. P. Martins. Abelian-Higgs Cosmic String Evolution with CUDA. *Astron. Comput.*, 32:100388, 2020.

[9] D. Forster. Dynamics of Relativistic Vortex Lines and their Relation to Dual Theory. *Nucl. Phys. B*, 81:84–92, 1974.

[10] A. Vilenkin and E. P. S. Shellard. *Cosmic Strings and Other Topological Defects*. Cambridge University Press, 7 2000.

[11] T. W. B. Kibble. Evolution of a system of cosmic strings. *Nucl. Phys. B*, 252:227, 1985. [Erratum: Nucl.Phys.B 261, 750 (1985)].

[12] C. J. Burden. Gravitational Radiation From a Particular Class of Cosmic Strings. *Phys. Lett. B*, 164:277–281, 1985.

[13] Lara Sousa. Cosmic strings and gravitational waves. *Gen. Rel. Grav.*, 56(9):105, 2024.

[14] J.J. Blanco-Pillado and Ken D. Olum. Electromagnetic radiation from superconducting string cusps. *Nuclear Physics B*, 599(1–2):435–445, April 2001.

[15] C. J. A. P. Martins and E. P. S. Shellard. Quantitative string evolution. *Physical Review D*, 54(4):2535–2556, August 1996.

[16] C. J. A. P. Martins and E. P. S. Shellard. Extending the velocity dependent one scale string evolution model. *Phys. Rev. D*, 65:043514, 2002.

[17] C. J. A. P. Martins and E. P. S. Shellard. String evolution with friction. *Phys. Rev. D*, 53:575–579, 1996.

[18] C. J. A. P. Martins, Patrick Peter, I. Yu. Rybak, and E. P. S. Shellard. Generalized velocity-dependent one-scale model for current-carrying strings. *Physical Review D*, 103(4), February 2021.

[19] T W B Kibble and Tanmay Vachaspati. Monopoles on strings. *Journal of Physics G: Nuclear and Particle Physics*, 42(9):094002, August 2015.

[20] C. J. A. P. Martins, Patrick Peter, I. Yu. Rybak, and E. P. S. Shellard. Charge-velocity-dependent one-scale linear model. *Phys. Rev. D*, 104(10):103506, 2021.

[21] C. J. A. P. Martins, E. P. S. Shellard, and J. P. P. Vieira. Models for small-scale structure of cosmic strings: Mathematical formalism. *Physical Review D*, 90(4), August 2014.

[22] J. P. P. Vieira, C. J. A. P. Martins, and E. P. S. Shellard. Models for small-scale structure on cosmic strings. ii. scaling and its stability. *Physical Review D*, 94(9), November 2016.

[23] M. F. Oliveira, A. Avgoustidis, and C. J. A. P. Martins. Cosmic string evolution with a conserved charge. *Physical Review D*, 85(8), April 2012.

[24] Thibault Damour and Alexander Vilenkin. Gravitational wave bursts from cusps and kinks on cosmic strings. *Phys. Rev. D*, 64:064008, 2001.

[25] Alexander Vilenkin and Tanmay Vachaspati. Electromagnetic Radiation from Superconducting Cosmic Strings. *Phys. Rev. Lett.*, 58:1041–1044, 1987.

[26] Brandon Carter and Patrick Peter. Supersonic string models for Witten vortices. *Phys. Rev. D*, 52:1744–1748, 1995.

[27] C. J. A. P. Martins, E. P. S. Shellard, and J. P. P. Vieira. Models for Small-Scale Structure on Cosmic Strings: Mathematical Formalism. *Phys. Rev. D*, 90(4):043518, 2014.

[28] I. Yu. Rybak, C. J. A. P. Martins, Patrick Peter, and E. P. S. Shellard. Cosmological evolution of Witten superconducting string networks. *Phys. Rev. D*, 107(12):123514, 2023.

[29] Ruth Durrer and Andrii Neronov. Cosmological magnetic fields: their generation, evolution and observation. *The Astronomy and Astrophysics Review*, 21(1), June 2013.

[30] Pranjal Trivedi, Kandaswamy Subramanian, and T. R. Seshadri. Primordial magnetic field limits from the cmb trispectrum: Scalar modes and planck constraints. *Physical Review D*, 89(4), February 2014.

[31] Oswaldo D. Miranda, Merav Opher, and Reuven Opher. Seed magnetic fields generated by primordial supernova explosions. *Monthly Notices of the Royal Astronomical Society*, 301(2):547–550, December 1998.

[32] Christos G Tsagas. Electromagnetic fields in curved spacetimes. *Classical and Quantum Gravity*, 22(2):393–407, December 2004.

[33] F. C. N. Q. Pimenta and C. J. A. P. Martins. Scaling solutions for current-carrying cosmic string networks. *Phys. Rev. D*, 110(2):023540, 2024.

[34] F. C. N. Q. Pimenta and C. J. A. P. Martins. Scaling solutions for current-carrying cosmic string networks. ii. biased solutions, 2025.

[35] Tanmay Vachaspati. Progress on cosmological magnetic fields. *Reports on Progress in Physics*, 84(7):074901, June 2021.

[36] J. R. C. C. C. Correia and C. J. A. P. Martins. Extending and Calibrating the Velocity dependent One-Scale model for Cosmic Strings with One Thousand Field Theory Simulations. *Phys. Rev. D*, 100(10):103517, 2019.

[37] J. P. Ostriker, Arthur Christopher Thompson, and Edward Witten. Cosmological Effects of Superconducting Strings. *Phys. Lett. B*, 180:231–239, 1986.